Institut für Theoretische Physik

Lattice Investigation of Heavy Meson Interactions

MASTER THESIS

Björn Fröhlich Wagenbach
born 12 January 1989

September 2014

Supervisor and 1st examiner	Prof. Marc Wagner
2nd examiner	Prof. Owe Philipsen

Eigenständigkeitserklärung

Gemäß §28 (12) der Ordnung des Fachbereichs Physik an der Johann Wolfgang Goethe-Universität für den Bachelor- und Masterstudiengang Physik vom 20.07.2011 versichere ich, dass ich die vorliegende Arbeit selbständig und ohne Benutzung anderer als der angegebenen Quellen und Hilfsmittel verfasst habe. Ferner erkläre ich, dass diese Arbeit, auch nicht auszugsweise, für eine andere Prüfung oder Studienleistung verwendet worden ist.

Frankfurt am Main, 17.09.2014 Björn Fröhlich Wagenbach

Zusammenfassung

In dieser Arbeit werden verschiedene Potentiale zwischen zwei statischen Antiquarks $\bar{Q}$, die jeweils von einem twisted mass-Quark mit endlicher Masse umgeben sind, berechnet. Ausgehend von den Resultaten für u- und d-Quarks, wird das Verhalten der Potentiale in Abhängigkeit der Quark-Masse untersucht. Dabei werden s- und c-Quarks betrachtet. Bezogen auf Hadronen, entspricht der erste Fall den Potentialen zwischen zwei B-Mesonen und der zweite Fall denen zwischen zwei B_s- bzw. B_c-Mesonen, wenn die statischen Antiquarks als b-Antiquarks betrachtet werden. Die Ergebnisse deuten darauf hin, dass für s- und c-Quarks, anders als für den Fall mit u- und d-Quarks, keine gebundenen Zustände existieren. Ein weiterer Aspekt dieser Arbeit ist die Erweiterung des Problems auf das Potential zwischen einem statischen Antiquark $\bar{Q}$ und einem statischen Quark Q, wieder jeweils von einem Quark oder Antiquark mit endlicher Masse umgeben. Ein erstes qualitatives Ergebnis ist die Tatsache, dass alle betrachteten $\bar{Q}Q$ Potentiale attraktiv sind. Für $\bar{Q}\bar{Q}$ traten sowohl attraktive als auch repulsive Potentiale auf.

Abstract

In this work different potentials between two static antiquarks $\bar{Q}$, each surrounded by a twisted mass quark of finite mass, are computed. Based on the results for u and d quarks, the behaviour of the potentials depending on the quark mass is investigated. Thereto s and c quarks are considered. Regarding hadrons, the first case corresponds to the potential between two B mesons and the second case to that between two B_s and B_c mesons, respectively, if the static antiquarks are considered as b antiquarks. Unlike the case with u and d quarks, the results indicate that there are no bound states for s and c quarks. Another aspect of this work is the extension of these investigations to the potential between a static antiquark $\bar{Q}$ and a static quark Q, each again surrounded by a quark or antiquark of finite mass. A first qualitative result is fact that all considered $\bar{Q}Q$ potentials are attractive. For $\bar{Q}\bar{Q}$ both attractive and repulsive potentials occurred.

Contents

Chapter 1

Introduction

Hadrons are clearly bound states of quarks and antiquarks, which are kept together by the strong force carried by gluons. Quantum Chromodynamics (QCD) is, as matters stand, the correct theory of the strong interaction. Since QCD allows more complex systems than mesons ($q\bar{q}$) and baryons (qqq), exotic hadrons have been searched for many years. One of these exotic hadrons is the tetraquark consisting of two quarks and two antiquarks ($qq\bar{q}\bar{q}$) and which existence was already claimed in the seventies [1]. In addition, there are several hadronic resonances which are tetraquark candidates, e.g. σ, κ, D_{s0}^{*}, ... [2].

However, the observation in experiments, the investigation using theoretical models and also the simulation in terms of lattice QCD is much more complex than for ordinary mesons and baryons.

Initial point of this thesis were the works [3–5], where the potential between two static-light mesons was investigated in order to provide information on the existence of a bound state, i.e. a tetraquark. Both static-light mesons were built up of an infinitely heavy (i.e. static) antiquark $\bar{Q}$ and a light quark $l \in \{u, d\}$ of finite mass. Regarding hadrons, this corresponds to the potential between two B mesons, since a static antiquark is a good approximation of a bottom antiquark $\bar{b}$, due to its significantly higher mass compared to the light quarks.

The investigation of the behaviour of these potentials depending on the quark mass is one of the two main goals of this work. As there was a clear indication for a bound state in one channel for $\bar{b}\bar{b}ll$, we are also looking for a heavier bound state with strange and charm quarks. This is of particular interest, since there are two possible scenarios concerning the existence of a bound state. Increasing the quark mass can either increase the chance of finding a bound state, because it is easier to reach binding with heavier constituents, or it can decrease the chance of finding a bound state, since the cloud formed by the quarks (i.e. their wave function) gets smaller which entails a smaller overlap of the two mesons implicating a more narrow potential.

The second main goal is to extend these investigations to a system consisting no longer of two static antiquarks but of one static antiquark and one static quark. Again regarding hadrons, this corresponds to the potential between a B meson and and $\bar{B}$ meson, if light quarks are considered. This case is experimentally more interesting, since due to conservation laws bottom quarks are always created in quark-antiquark pairs. Hence, to get two bottom quarks one would have to create two bottom quark-antiquark pairs and then separate the two quarks from the antiquarks. Whereas to get a $\bar{b}b\bar{l}l$ system, the creation of only one bottom quark-antiquark pair is sufficient.

Nevertheless, such a system involves some new difficulties. For instance, the light quark and the light antiquark can annihilate resulting in a $\bar{Q}Q$ pair connected by a gluonic string. One also has to distinguish in a $\bar{b}b\bar{l}l$ system two cases of essentially non-interacting mesons, i.e. $B\bar{B}$ and the case of a pion ($l\bar{l}$) together with the mentioned by gluons connected $\bar{Q}Q$ pair.

In the following, we want to give a short outline of this thesis. We start with some theoretical basics, which are relevant to comprehend the calculations and results of this work. The next chapter deals with the corresponding technical realisation in terms of lattice computations. This is then followed by the results of the numerical computations. Finally, the last chapter gives a summary of this thesis and an outlook on possible further work.

Chapter 2

Theoretical foundations

2.1 Notation

Both the colour indices and the flavours are denoted by lower case letters in the upper indices. To distinguish between them, the flavours are enclosed in brackets and, in addition, always written in front of the colour indices. Spinor indices are denoted by capital letters in the lower indices, e.g.

$$\psi_A^{(u)b}(\vec{r}) \tag{2.1}$$

describes a fermionic field ψ (e.g. a quark field) located at space point $\vec{r}$ with spinor index A, colour index b and flavour u.

However, in some cases not all of the indices are shown for the purpose of a more convenient reading.

Moreover, we will denote fermionic fields in the (pseudo) physical basis with $\{\psi, \bar{\psi}\}$ and for the twisted basis we will use $\{\chi, \bar{\chi}\}$.

2.2 Twisted mass lattice QCD

For a detailed introduction to twisted mass lattice QCD (tmLQCD) we refer to [6]. This section is just meant to give a rough overview.

The twisted mass QCD action for $N_f = 2$ degenerate light quarks $\chi^{(l)} \in \{\chi^{(u)}, \chi^{(d)}\}$ in a continuum like version reads:

$$S_{\text{light}}\left[\chi, \bar{\chi}, A\right] = \int d^4x \; \bar{\chi}^{(l)}\Big(\gamma_\mu D_\mu + m_q + i\mu_q\gamma_5\tau^3 - \frac{a}{2}\,\Box\Big)\chi^{(l)}\,, \tag{2.2}$$

where D_μ denotes the covariant derivative, A_μ the gauge field and a the lattice spacing within the so called Wilson term. m_q is the untwisted quark mass, μ_q the twisted quark mass and τ^3 the third Pauli matrix acting in flavour space.

A part of the calculations in this work is also based on $N_f = 2+1+1$ flavours, where (2.2) for the light (u,d) doublet and

$$S_{\text{heavy}}\left[\chi, \bar{\chi}, A\right] = \int d^4x \; \bar{\chi}^{(h)} \Big(\gamma_\mu D_\mu + m_q + i\mu_\sigma \gamma_5 \tau^1 + \mu_\delta \tau^3 - \frac{a}{2} \Box \Big) \chi^{(h)} \tag{2.3}$$

for the heavy non-degenerate (s,c) sea quark doublet, with $\chi^{(h)} \in \{\chi^{(s)}, \chi^{(c)}\}$, was used.

The corresponding discretised twisted mass lattice actions $S_{\text{light}}\left[\chi, \bar{\chi}, U\right]$ and $S_{\text{heavy}}\left[\chi, \bar{\chi}, U\right]$, with the link variables U, are shown in [7].

In order to avoid a flavour mixing of the strange and charm quarks [8], we used the degenerate action of (2.2) in the corresponding valence sectors. This yields two degenerate twisted mass doublets (c^+,c^-) and (s^+,s^-) by changing $\chi^{(l)} \to \chi^{(s)} \in \{\chi^{(s^+)}, \chi^{(s^-)}\}$ and $\chi^{(l)} \to \chi^{(c)} \in \{\chi^{(c^+)}, \chi^{(c^-)}\}$, respectively.

Throughout this work we always work in euclidean space-time and use the chiral representation of the Dirac matrices

$$\gamma_0 = \begin{pmatrix} 0 & -1 \\ -1 & 0 \end{pmatrix}, \quad \gamma_j = \begin{pmatrix} 0 & -i\tau^j \\ +i\tau^j & 0 \end{pmatrix}, \tag{2.4}$$

with the Pauli matrices

$$\tau^1 = \begin{pmatrix} 0 & +1 \\ +1 & 0 \end{pmatrix}, \quad \tau^2 = \begin{pmatrix} 0 & -i \\ +i & 0 \end{pmatrix}, \quad \tau^3 = \begin{pmatrix} +1 & 0 \\ 0 & -1 \end{pmatrix}. \tag{2.5}$$

The (pseudo) physical basis $\{\psi, \bar{\psi}\}$ is related to the twisted basis $\{\chi, \bar{\chi}\}$ by a so called twist rotation:

$$\begin{aligned} \psi^{(u)} &= e^{+i\frac{\omega}{2}\gamma_5} \chi^{(u)} \implies \bar{\psi}^{(u)} = \bar{\chi}^{(u)} e^{+i\frac{\omega}{2}\gamma_5} \\ \psi^{(d)} &= e^{-i\frac{\omega}{2}\gamma_5} \chi^{(d)} \implies \bar{\psi}^{(d)} = \bar{\chi}^{(d)} e^{-i\frac{\omega}{2}\gamma_5} \end{aligned} \tag{2.6}$$

Our calculations are done at maximal twist, i.e. $\omega = \frac{\pi}{2}$. This involves an automatic O(a) improvement of the physical observables [9].

2.2.1 Relation between $\Gamma^{(\mathrm{ppb})}$ and $\Gamma^{(\mathrm{tb})}$

With (2.6) we easily obtain the following relations:

$$\begin{aligned}
\psi^{T(u)}\,\Gamma^{(\mathrm{ppb})}\,\bar{\psi}^{T(u)} &= \chi^{T(u)} e^{+i\frac{\omega}{2}\gamma_5}\,\Gamma^{(\mathrm{ppb})}\,e^{+i\frac{\omega}{2}\gamma_5}\bar{\chi}^{(u)} = \chi^{T(u)}\,\Gamma^{(\mathrm{tb})}_{u\bar{u}}\,\bar{\chi}^{(u)} \\
\psi^{T(d)}\,\Gamma^{(\mathrm{ppb})}\,\bar{\psi}^{T(d)} &= \chi^{T(d)} e^{-i\frac{\omega}{2}\gamma_5}\,\Gamma^{(\mathrm{ppb})}\,e^{-i\frac{\omega}{2}\gamma_5}\bar{\chi}^{(d)} = \chi^{T(d)}\,\Gamma^{(\mathrm{tb})}_{d\bar{d}}\,\bar{\chi}^{(d)} \\
\psi^{T(u)}\,\Gamma^{(\mathrm{ppb})}\,\bar{\psi}^{T(d)} &= \chi^{T(u)} e^{+i\frac{\omega}{2}\gamma_5}\,\Gamma^{(\mathrm{ppb})}\,e^{-i\frac{\omega}{2}\gamma_5}\bar{\chi}^{(d)} = \chi^{T(u)}\,\Gamma^{(\mathrm{tb})}_{u\bar{d}}\,\bar{\chi}^{(d)} \\
\psi^{T(d)}\,\Gamma^{(\mathrm{ppb})}\,\bar{\psi}^{T(u)} &= \chi^{T(d)} e^{-i\frac{\omega}{2}\gamma_5}\,\Gamma^{(\mathrm{ppb})}\,e^{+i\frac{\omega}{2}\gamma_5}\bar{\chi}^{(u)} = \chi^{T(d)}\,\Gamma^{(\mathrm{tb})}_{d\bar{u}}\,\bar{\chi}^{(u)}
\end{aligned} \tag{2.7}$$

Hence, we are able to establish a relation between the Γ-matrices in the (pseudo) physical basis $\Gamma^{(\mathrm{ppb})}$ and the Γ-matrices in the twisted basis $\Gamma^{(\mathrm{tb})}$, which is shown in Table 2.1.

$\Gamma^{(\mathrm{ppb})}$	$\Gamma^{(\mathrm{tb})}_{u\bar{u}}$	$\Gamma^{(\mathrm{tb})}_{d\bar{d}}$	$\Gamma^{(\mathrm{tb})}_{u\bar{d}}$	$\Gamma^{(\mathrm{tb})}_{d\bar{u}}$
γ_5	$+i$	$-i$	$+\gamma_5$	$+\gamma_5$
$\gamma_0\gamma_5$	$+\gamma_0\gamma_5$	$+\gamma_0\gamma_5$	$-i\gamma_0$	$+i\gamma_0$
1	$+i\gamma_5$	$-i\gamma_5$	$+1$	$+1$
γ_0	$+\gamma_0$	$+\gamma_0$	$-i\gamma_0\gamma_5$	$+i\gamma_0\gamma_5$
γ_3	$+\gamma_3$	$+\gamma_3$	$-i\gamma_3\gamma_5$	$+i\gamma_3\gamma_5$
$\gamma_0\gamma_3$	$+i\gamma_0\gamma_3\gamma_5$	$-i\gamma_0\gamma_3\gamma_5$	$+\gamma_0\gamma_3$	$+\gamma_0\gamma_3$
$\gamma_3\gamma_5$	$+\gamma_3\gamma_5$	$+\gamma_3\gamma_5$	$-i\gamma_3$	$+i\gamma_3$
$\gamma_0\gamma_3\gamma_5$	$+i\gamma_0\gamma_3$	$-i\gamma_0\gamma_3$	$+\gamma_0\gamma_3\gamma_5$	$+\gamma_0\gamma_3\gamma_5$
γ_1	$+\gamma_1$	$+\gamma_1$	$-i\gamma_1\gamma_5$	$+i\gamma_1\gamma_5$
γ_2	$+\gamma_2$	$+\gamma_2$	$-i\gamma_2\gamma_5$	$+i\gamma_2\gamma_5$
$\gamma_0\gamma_1$	$+i\gamma_0\gamma_1\gamma_5$	$-i\gamma_0\gamma_1\gamma_5$	$+\gamma_0\gamma_1$	$+\gamma_0\gamma_1$
$\gamma_0\gamma_2$	$+i\gamma_0\gamma_2\gamma_5$	$-i\gamma_0\gamma_2\gamma_5$	$+\gamma_0\gamma_2$	$+\gamma_0\gamma_2$
$\gamma_1\gamma_5$	$+\gamma_1\gamma_5$	$+\gamma_1\gamma_5$	$-i\gamma_1$	$+i\gamma_1$
$\gamma_2\gamma_5$	$+\gamma_2\gamma_5$	$+\gamma_2\gamma_5$	$-i\gamma_2$	$+i\gamma_2$
$\gamma_0\gamma_1\gamma_5$	$+i\gamma_0\gamma_1$	$-i\gamma_0\gamma_1$	$+\gamma_0\gamma_1\gamma_5$	$+\gamma_0\gamma_1\gamma_5$
$\gamma_0\gamma_2\gamma_5$	$+i\gamma_0\gamma_2$	$-i\gamma_0\gamma_2$	$+\gamma_0\gamma_2\gamma_5$	$+\gamma_0\gamma_2\gamma_5$

Table 2.1: Relation between the Γ-matrices in the (pseudo) physical basis and the twisted basis

The red coloured Γ-matrices are those who change after the performed twist rotation. As can be seen, not only the structure of these Γ-matrices changes, but also their sign. The consequence is that the relative sign between some flavour combinations changes, e.g. $u\bar{u} + d\bar{d} \to u\bar{u} - d\bar{d}$. We have to keep this in mind for the further considerations.

2.3 Trial states

To get a trial state $|\psi\rangle$ with specific quantum numbers $I(J^P)$, one has to construct an operator $\mathcal{O}$, which creates these quantum numbers by acting on the QCD vacuum $|\Omega\rangle$:

$$|\psi\rangle = \mathcal{O}\,|\Omega\rangle \tag{2.8}$$

Hence, such operators $\mathcal{O}$ are called creation operators and build the basis for the computation of the correlation function

$$\begin{aligned} C(t) &\equiv \langle\Omega|\mathcal{O}^\dagger(t)\,\mathcal{O}(0)\,|\Omega\rangle \\ &= \sum_{n=0}^{\infty} \langle\Omega|\, e^{+Ht}\mathcal{O}^\dagger(0)e^{-Ht}\,|n\rangle\langle n|\,\mathcal{O}(0)\,|\Omega\rangle \\ &= \sum_{n=0}^{\infty} \underbrace{\left|\langle n|\mathcal{O}|\Omega\rangle\right|^2}_{=|a_n|^2} \exp\Big(-\underbrace{(E_n - E_\Omega)}_{=m_n}\,t\Big) \overset{t\gg 1}{\approx} |a_0|^2 e^{-m_0\,t}, \end{aligned} \tag{2.9}$$

from which we can extract the effective mass

$$m_{\text{eff}}(t) \equiv \frac{1}{a}\log\left(\frac{C(t)}{C(t+a)}\right) \overset{t\gg 1}{\approx} m\,. \tag{2.10}$$

Computing $m_{\text{eff}}(t)$ for different separations of the two considered mesons will then lead to the potential we are looking for.

For a better comparison with [3, 4] we focus in this section only on light quarks, i.e. flavours $l \in \{u, d\}$. Nevertheless, these considerations hold also for s and c quarks, which will be considered later.[1]

2.3.1 Static-light mesons

Starting point are the static-light mesons built up either from a static quark Q and an antiquark $\bar{\psi}$ or a static antiquark $\bar{Q}$ and a quark ψ, with $\psi \in \{u, d\}$ and a finite mass. These mesons can be labelled by parity $\mathscr{P} = \pm$, the z-component of isospin $I_z = \pm 1$ and, since non-trivial gluonic excitations are not considered, i.e. $j = \frac{1}{2}$, the z-component of the light quark spin $j_z = \pm\frac{1}{2}$. The lightest static-light meson has $\mathscr{P} = -$ and is denoted by S and the parity partner with $\mathscr{P} = +$ is denoted by P_-. Regarding $\bar{Q}\psi$ and identifying $\bar{Q}$ with $\bar{b}$, S corresponds to B/B^* and P_- to B_0^*/B_1^*, listed in [10]. For $Q\bar{\psi}$, S corresponds to $\bar{B}/\bar{B}^*$ and P_- to $\bar{B}_0^*/\bar{B}_1^*$, respectively.

1 Then $u \to s^+/c^+$ and $d \to s^-/c^-$, where $+/-$ describe the sign within the twist rotation, cf. (2.6).

The static-light meson trial states have the following structure:

$$\bar{Q}\Gamma\psi|\Omega\rangle \quad \text{and} \quad \bar{\psi}\Gamma Q|\Omega\rangle, \tag{2.11}$$

with $\Gamma \in \{\gamma_5, \gamma_0\gamma_5, \gamma_j, \gamma_0\gamma_j\}$ for the S and $\Gamma \in \{1, \gamma_0, \gamma_j\gamma_5, \gamma_0\gamma_j\gamma_5\}$ for the P_- state.

For a more detailed discussion of static-light mesons see [11, 12].

2.3.2 BB potentials

As already mentioned in the introduction, we are interested in the potential between two static-light mesons as a function of the separation. Here and in the following the separation is denoted by R and the axis of separation is without loss of generality chosen to be the z-axis, where the two static antiquarks $\bar{Q}$ are located at $\vec{r}_1 = (0, 0, +\frac{R}{2})^T$ and $\vec{r}_2 = (0, 0, -\frac{R}{2})^T$, respectively. The static quarks are surrounded by the light quarks, which have no fixed position. This means $\vec{r}_1$ and $\vec{r}_2$ do also define the position of the B mesons.

For the BB system the following trial states were used:

$$(\mathcal{C}\Gamma)_{AB}\ \bar{Q}^a_C(\vec{x})\ \psi^{(f_1)a}_A(\vec{x})\ \bar{Q}^b_C(\vec{y})\ \psi^{(f_2)b}_B(\vec{y})\ |\Omega\rangle, \tag{2.12}$$

where $\mathcal{C} = \gamma_0\gamma_2$ is the charge conjugation matrix and the notation shown in section 2.1 was used.

These states can be labelled by the isospin $I \in \{0, 1\}$, its z-component $I_z \in \{-1, 0, +1\}$, the absolute value of the z-component of the light quark spin $|j_z| \in \{0, 1\}$, the parity $\mathscr{P} = \pm$ and the "x-parity" $\mathscr{P}_x = \pm$, which is a reflection along the x-axis.

For more information cf. [3, 4] and also Appendix A, where the different quantum numbers are listed. Moreover, we will give a detailed discussion of the different symmetries and quantum numbers of $B\bar{B}$ systems in section 2.6.

2.3.3 $B\bar{B}$ potentials

We are now regarding the completely new case of a $B\bar{B}$ system, which means we have to replace one of the B mesons by a $\bar{B}$ meson. Starting from (2.12), we used the following $B\bar{B}$ trial states

$$\Gamma_{AB}\,\tilde{\Gamma}_{CD}\ \bar{Q}^a_C(\vec{x})\ \psi^{(f_1)a}_A(\vec{x})\ \bar{\psi}^{(f_2)b}_B(\vec{y})\ Q^b_D(\vec{y})\ |\Omega\rangle \tag{2.13}$$

where due to the new quark-antiquark structure the charge conjugation matrix C is not needed any longer and therefore dropped. In addition, although there are no interactions involving the static spin, we have to consider the connection between the static quark and the static antiquark in spin space, i.e. we inserted a $\tilde{\Gamma}$ matrix. The reson for this will be explained later.

(2.13) leads to the following correlation function, where $\Gamma(t)$ denotes the Γ matrix within the operator $\mathcal{O}(t)$ and $\Gamma(0)$ the Γ matrix within the operator $\mathcal{O}(0)$, not to be confused with a time dependence of the Γ matrices:

$$\begin{aligned}
C(t) &= \langle\Omega|\mathcal{O}^\dagger(t)\mathcal{O}(0)|\Omega\rangle \\
&= (\gamma_0\Gamma^*(t)\gamma_0)_{AB}\ (\gamma_0\tilde{\Gamma}^*\gamma_0)_{CD}\ \Gamma(0)_{EF}\ \tilde{\Gamma}_{GH}\ \langle\Omega|\bar{Q}_D^b(\vec{y},t)\ \psi_B^{(2)b}(\vec{y},t)\ \bar{\psi}_A^{(1)a}(\vec{x},t)\ Q_C^a(\vec{x},t) \\
&\quad \bar{Q}_G^c(\vec{x},0)\ \psi_E^{(1)c}(\vec{x},0)\ \bar{\psi}_F^{(2)d}(\vec{y},0)\ Q_H^d(\vec{y},0)|\Omega\rangle \\
&= (\gamma_0\Gamma^*(t)\gamma_0)_{AB}\ (\gamma_0\tilde{\Gamma}^*\gamma_0)_{CD}\ \Gamma(0)_{EF}\ \tilde{\Gamma}_{GH}\ \langle\Omega|\,\mathrm{Tr}_{\mathrm{col}}\Big[Q_C(\vec{x},t)\ \bar{Q}_G(\vec{x},0)\ \psi_E^{(1)}(\vec{x},0)\ \bar{\psi}_A^{(1)}(\vec{x},t)\Big] \\
&\quad \mathrm{Tr}_{\mathrm{col}}\Big[Q_H(\vec{y},0)\ \bar{Q}_D(\vec{y},t)\ \psi_B^{(2)}(\vec{y},t)\ \bar{\psi}_F^{(2)}(\vec{y},0)\Big]|\Omega\rangle \\
&= +e^{-2Mt}\ (\gamma_0\Gamma^*(t)\gamma_0)_{AB}\ \Gamma(0)_{EF}\ (\gamma_0\tilde{\Gamma}^\dagger\gamma_0)_{DC}\left(\frac{1+\gamma_0}{2}\right)_{CG}\tilde{\Gamma}_{GH}\left(\frac{1-\gamma_0}{2}\right)_{HD} \\
&\quad \Big\langle\mathrm{Tr}_{\mathrm{col}}\Big[U(\vec{x},t;\vec{x},0)\ (D^{-1})_{EA}^{(\psi_1)}(\vec{x},0;\vec{x},t)\Big]\ \mathrm{Tr}_{\mathrm{col}}\Big[U(\vec{y},0;\vec{y},t)\ (D^{-1})_{BF}^{(\psi_2)}(\vec{y},t;\vec{y},0)\Big]\Big\rangle \\
&= +e^{-2Mt}\ (\gamma_0\Gamma^*(t)\gamma_0)_{AB}\ (\Gamma(0)^T)_{DC}\ \mathrm{Tr}_{\mathrm{spin}}\Big[\gamma_0\tilde{\Gamma}^\dagger\gamma_0\left(\frac{1+\gamma_0}{2}\right)\tilde{\Gamma}\left(\frac{1-\gamma_0}{2}\right)\Big] \\
&\quad \Big\langle\mathrm{Tr}_{\mathrm{col}}\Big[U(\vec{x},t;\vec{x},0)\ (D^{-1})_{CA}^{(\psi_1)}(\vec{x},0;\vec{x},t)\Big]\ \mathrm{Tr}_{\mathrm{col}}\Big[U(\vec{y},0;\vec{y},t)\ (D^{-1})_{BD}^{(\psi_2)}(\vec{y},t;\vec{y},0)\Big]\Big\rangle\,, \qquad (2.14)
\end{aligned}$$

where in the second last step the light quark propagator D^{-1} was inserted and where $\langle ...\rangle$ denotes a path integral over the gauge fields A. Within the scope of heavy quark effective theory it can be shown for the static quark propagator $\mathcal{Q}^{-1}$ that [11]

$$\begin{aligned}
(\mathcal{Q}^{-1})_{AB}^{ab}(x;y) = \delta(\vec{x}-\vec{y})U^{ab}(\vec{x},x_0;\vec{y},y_0)\Big(&\Theta(y_0-x_0)\left(\frac{1-\gamma_0}{2}\right)_{AB}e^{-M(y_0-x_0)} \\
&+\Theta(x_0-y_0)\left(\frac{1+\gamma_0}{2}\right)_{AB}e^{-M(x_0-y_0)}\Big),
\end{aligned} \qquad (2.15)$$

which was also used and where

$$U(\vec{x},x_0;\vec{y},y_0) = P\left[\exp\left(\pm i\int_{x_0}^{y_0}\mathrm{d}z_0 A_0(\vec{x},z_0)\right)\right], \qquad (2.16)$$

with P denoting a path-ordered integration.

Moreover, (2.14) shows that the following condition has to be fulfilled:

$$\left\{\tilde{\Gamma},\gamma_0\right\} = 0 \iff \tilde{\Gamma}\gamma_0 = -\gamma_0\tilde{\Gamma} \qquad (2.17)$$

Otherwise the correlator would vanish, since:

$$\left(\frac{1 \pm \gamma_0}{2}\right)\left(\frac{1 \mp \gamma_0}{2}\right) = 0 \tag{2.18}$$

A possible choice is $\tilde{\Gamma} \in \{\gamma_5, \gamma_0\gamma_5, \gamma_3, \gamma_0\gamma_3, \gamma_1, \gamma_2, \gamma_0\gamma_1, \gamma_0\gamma_2\}$, which yields:

$$\mathrm{Tr}_{\mathrm{spin}}\left[\gamma_0\tilde{\Gamma}^\dagger\gamma_0\left(\frac{1+\gamma_0}{2}\right)\tilde{\Gamma}\left(\frac{1-\gamma_0}{2}\right)\right] = -2 \tag{2.19}$$

by using the following relations:

$$\begin{gathered}\tilde{\Gamma}^\dagger\tilde{\Gamma} = 1 \\ \left(\frac{1 \pm \gamma_0}{2}\right)\left(\frac{1 \pm \gamma_0}{2}\right) = \frac{1 \pm \gamma_0}{2} \\ \mathrm{Tr}\left(\frac{1 \pm \gamma_0}{2}\right) = 2\end{gathered} \tag{2.20}$$

Consequently, the correlation function (2.14) becomes the following:

$$\begin{aligned}C(t) = &-2e^{-2Mt}\ (\gamma_0\Gamma^*(t)\gamma_0)_{AB}\ (\Gamma^T(0))_{DC} \\ &\left\langle \mathrm{Tr}_{\mathrm{col}}\Big[U(\vec{x},t;\vec{x},0)\ (D^{-1})^{(\psi_1)}_{CA}(\vec{x},0;\vec{x},t)\Big]\ \mathrm{Tr}_{\mathrm{col}}\Big[U(\vec{y},0;\vec{y},t)\ (D^{-1})^{(\psi_2)}_{BD}(\vec{y},t;\vec{y},0)\Big]\right\rangle\end{aligned} \tag{2.21}$$

As one might have expected, the $\tilde{\Gamma}$ matrix drops out and has no influence on the correlation function and therefore, no influence on the potentials we are interested in.[2]

To estimate the correlation function (2.21), we have to compute the link variables U given in (2.16) and the light quark propagators D^{-1} which is discussed in section 3.1.

2.4 A closer look at isospin

The light quarks can be combined to isospin $I = 0$ and $I = 1$. For u and d quarks this is done in the following way:

$$\begin{aligned}I = 0: &\quad ud - du \\ I = 1: &\quad uu,\ dd,\ ud + du\end{aligned}$$

2 Inserting a $\tilde{\Gamma}$ matrix into the BB trial state yields the same conclusion, whereby in that case one has to choose $\tilde{\Gamma} \in \{1, \gamma_0, \gamma_3\gamma_5, \gamma_1\gamma_2, \gamma_1\gamma_5, \gamma_2\gamma_5, \gamma_2\gamma_3, \gamma_1\gamma_3\}$. Hence, $\tilde{\Gamma} = 1$ is a possible choice and made in (2.12).

But now we are interested in the coupling of a quark and an antiquark. Therefore we have to check the transformation of antiquarks under isospin rotation:

$$\begin{pmatrix} u \\ d \end{pmatrix} \to e^{i\alpha^a \frac{\tau^a}{2}} \begin{pmatrix} u \\ d \end{pmatrix} \quad \Longrightarrow \quad \begin{pmatrix} \bar{u} \\ \bar{d} \end{pmatrix}^{\mathrm{T}} \to \begin{pmatrix} \bar{u} \\ \bar{d} \end{pmatrix}^{\mathrm{T}} e^{-i\alpha^a \frac{\tau^a}{2}} \tag{2.22}$$

To get an equal structure for the antiquarks we have to transpose the result, which gives us:

$$\begin{pmatrix} \bar{u} \\ \bar{d} \end{pmatrix} \to e^{-i\alpha^a \frac{(\tau^a)^{\mathrm{T}}}{2}} \begin{pmatrix} \bar{u} \\ \bar{d} \end{pmatrix} = e^{-i\alpha^a \frac{(\tau^a)^{\mathrm{T}}}{2}} \tau^2 \tau^2 \begin{pmatrix} \bar{u} \\ \bar{d} \end{pmatrix} = \tau^2 e^{i\alpha^a \frac{\tau^a}{2}} \tau^2 \begin{pmatrix} \bar{u} \\ \bar{d} \end{pmatrix} \tag{2.23}$$

Multiplying this equation by $\pm i\tau^2$ yields:

$$\begin{pmatrix} \pm\bar{d} \\ \mp\bar{u} \end{pmatrix} \to e^{i\alpha^a \frac{\tau^a}{2}} \begin{pmatrix} \pm\bar{d} \\ \mp\bar{u} \end{pmatrix} \tag{2.24}$$

from which we can conclude by comparison with the left part of (2.22) and neglecting (without loss of generality) global minus sign:

$$\begin{aligned} I = 0: &\quad ud - du \mathrel{\widehat{=}} u\bar{u} + d\bar{d} \\ I = 1: &\quad uu,\ dd,\ ud + du \mathrel{\widehat{=}} u\bar{d},\ d\bar{u},\ u\bar{u} - d\bar{d} \end{aligned}$$

In this case "$\widehat{=}$" denotes same transformation laws.

2.5 Interpretation in terms of static-light mesons

To identify the meson content of the different $B\bar{B}$ operators introduced in (2.13) one has to use the parity and the spin projectors given in the following way:

Parity projectors:

$$P_{\mathscr{P}=+} = \frac{1+\gamma_0}{2}\ , \quad P_{\mathscr{P}=-} = \frac{1-\gamma_0}{2} \tag{2.25}$$

Spin projectors:

$$P_{j_z=\uparrow} = \frac{1+i\gamma_0\gamma_3\gamma_5}{2}\ , \quad P_{j_z=\downarrow} = \frac{1-i\gamma_0\gamma_3\gamma_5}{2} \tag{2.26}$$

These projectors act on light quark fields, but we are interested in the quantum numbers of static-light mesons. Since the spin of static-light mesons is only carried by the light quarks [12], the spin

projectors (2.26) have obviously the same effect on static-light mesons. But we have to check if this also holds for the parity projectors (2.25):

The correlation function of the studied $B\bar{B}$ system has roughly the form $(\bar{Q}\,\Gamma\,q)(\bar{q}\,\Gamma\,Q)$. For an easier understanding, we will first focus on only one meson term, the second term. Looking at the propagator for static quarks (2.15) this term can be replaced by:

$$\left(\bar{q}\;\Gamma\;\frac{1-\gamma_0}{2}\;Q\right) \tag{2.27}$$

If we now consider a light antiquark field with *positive* parity, replacing $\bar{q}$ by $\bar{q}\,\frac{1+\gamma_0}{2}$ does not change anything. The correlation function then reads:

$$\left(\bar{q}\;\frac{1+\gamma_0}{2}\;\Gamma\;\frac{1-\gamma_0}{2}\;Q\right) \tag{2.28}$$

By inserting γ combinations which belong to *positive* meson parity, i.e $1, \gamma_0, \gamma_j\gamma_5$ or $\gamma_0\gamma_j\gamma_5$, this term vanishes (cf. (2.18)). This would mean that the parity of the $(\bar{q}\,\Gamma\,Q)$ meson is *negative* if the light antiquark field has *positive* parity. If a γ combination belonging to *negative* meson parity is inserted, i.e $\gamma_5, \gamma_0\gamma_5, \gamma_j$ or $\gamma_0\gamma_j$, one comes to the same conclusion that the parity of the $(\bar{q}\,\Gamma\,Q)$ meson is the inverse of the parity of light antiquark field.

Also if one considers a light antiquark field with *negative* parity this presumption seems to be true. Therefore we have to use the *negative* parity projector of the light quark fields $P_{\mathscr{P}=-}$ to get a *positive* meson parity for $(\bar{q}\,\Gamma\,Q)$ and vice versa. We have to keep this in mind for the following considerations.

Regarding the $(\bar{Q}\,\Gamma\,q)$ meson and following the same steps, yields that the parity of this meson is equal to that of the light quark field. Hence, we can use the parity projectors (2.25) for this meson in the same way as for light quark fields.

To extract the meson content of the $B\bar{B}$ system we first have to write the projectors in terms of eigenvectors corresponding to eigenvalues unequal to 0:

$$\begin{aligned}
P_{\mathscr{P}=+}P_{j_z=\uparrow} &= \vec{v}_{\mathscr{P}=+,j_z=\uparrow}\left(\vec{v}_{\mathscr{P}=+,j_z=\uparrow}\right)^\dagger \\
P_{\mathscr{P}=+}P_{j_z=\downarrow} &= \vec{v}_{\mathscr{P}=+,j_z=\downarrow}\left(\vec{v}_{\mathscr{P}=+,j_z=\downarrow}\right)^\dagger \\
P_{\mathscr{P}=-}P_{j_z=\uparrow} &= \vec{v}_{\mathscr{P}=-,j_z=\uparrow}\left(\vec{v}_{\mathscr{P}=-,j_z=\uparrow}\right)^\dagger \\
P_{\mathscr{P}=-}P_{j_z=\downarrow} &= \vec{v}_{\mathscr{P}=-,j_z=\downarrow}\left(\vec{v}_{\mathscr{P}=-,j_z=\downarrow}\right)^\dagger
\end{aligned} \tag{2.29}$$

with

$$\begin{aligned}\vec{v}_{\mathscr{P}=+,j_z=\uparrow} &= \frac{1}{\sqrt{2}}(+1,0,-1,0)^T, \quad \vec{v}_{\mathscr{P}=+,j_z=\downarrow} = \frac{1}{\sqrt{2}}(0,+1,0,-1)^T \\ \vec{v}_{\mathscr{P}=-,j_z=\uparrow} &= \frac{1}{\sqrt{2}}(+1,0,+1,0)^T, \quad \vec{v}_{\mathscr{P}=-,j_z=\downarrow} = \frac{1}{\sqrt{2}}(0,+1,0,+1)^T\end{aligned} \tag{2.30}$$

One can easily show, that

$$1 = P_{\mathscr{P}=+}P_{j_z=\uparrow} + P_{\mathscr{P}=+}P_{j_z=\downarrow} + P_{\mathscr{P}=-}P_{j_z=\uparrow} + P_{\mathscr{P}=-}P_{j_z=\downarrow} \tag{2.31}$$

is fulfilled.

Inserting this identity into the light spin coupling of the $B\bar{B}$ creation operator yields:

$$\begin{aligned}\psi^T \Gamma \bar{\psi}^T &= -\bar{\psi}\,\Gamma^T \psi \\ &= -\sum_{\substack{P_1=\pm \\ j_1=\uparrow/\downarrow}} \sum_{\substack{P_2=\pm \\ j_2=\uparrow/\downarrow}} \bar{\psi}\ \vec{v}_{\mathscr{P}=P_1,j_z=j_1} \underbrace{\left(\vec{v}_{\mathscr{P}=P_1,j_z=j_1}\right)^\dagger \Gamma^T \vec{v}_{\mathscr{P}=P_2,j_z=j_2}}_{=:\ -c_{P_1,j_1,P_2,j_2}} \left(\vec{v}_{\mathscr{P}=P_2,j_z=j_2}\right)^\dagger \psi\end{aligned} \tag{2.32}$$

where the coefficients c_{P_1,j_1,P_2,j_2} represent the static-light meson content. According to the previous considerations the meson $(\bar{Q}\,\Gamma\,q)$ has the quantum numbers $\mathscr{P} = P_2$ and $j_z = j_2$, and the meson $(\bar{q}\,\Gamma\,Q)$ has the quantum numbers $\mathscr{P} = -P_1$ and $j_z = j_1$.

The meson content of the $B\bar{B}$ system depending on the Γ choice in the (pseudo) physical basis is listed in Table 2.2. As introduced in subsection 2.3.1, S indicates a static light meson with $\mathscr{P} = -$ and P_- (here abbreviated P) a static-light meson with $\mathscr{P} = +$. The light cloud angular momentum is denoted by $\uparrow$ and $\downarrow$.[3]

These considerations are very helpful, since for sufficiently large separations the $B\bar{B}$ system can be treated as two non-interacting $B/\bar{B}$ mesons. Hence, the potentials should saturate at a plateau with the value of two times the corresponding meson mass.

For instance, the $B\bar{B}$ system with the γ-combination $\gamma_5 - \gamma_0\gamma_5$ only contains S mesons. Therefore the related potential should saturate at $2\,m(S)$. This will also be used to normalise the potentials.

3 The corresponding table for BB systems can be taken from Appendix A.

Γ (pseudo) physical	meson content
γ_5	$+S_\uparrow S_\uparrow + S_\downarrow S_\downarrow + P_\uparrow P_\uparrow + P_\downarrow P_\downarrow$
$\gamma_0\gamma_5$	$-S_\uparrow S_\uparrow - S_\downarrow S_\downarrow + P_\uparrow P_\uparrow + P_\downarrow P_\downarrow$
1	$+S_\uparrow P_\uparrow + S_\downarrow P_\downarrow + P_\uparrow S_\uparrow + P_\downarrow S_\downarrow$
γ_0	$+S_\uparrow P_\uparrow + S_\downarrow P_\downarrow - P_\uparrow S_\uparrow - P_\downarrow S_\downarrow$
γ_3	$+iS_\uparrow S_\uparrow - iS_\downarrow S_\downarrow - iP_\uparrow P_\uparrow + iP_\downarrow P_\downarrow$
$\gamma_0\gamma_3$	$-iS_\uparrow S_\uparrow + iS_\downarrow S_\downarrow - iP_\uparrow P_\uparrow + iP_\downarrow P_\downarrow$
$\gamma_3\gamma_5$	$-iS_\uparrow P_\uparrow + iS_\downarrow P_\downarrow + iP_\uparrow S_\uparrow - iP_\downarrow S_\downarrow$
$\gamma_0\gamma_3\gamma_5$	$-iS_\uparrow P_\uparrow + iS_\downarrow P_\downarrow - iP_\uparrow S_\uparrow + iP_\downarrow S_\downarrow$
γ_1	$+iS_\uparrow S_\downarrow + iS_\downarrow S_\uparrow - iP_\uparrow P_\downarrow - iP_\downarrow P_\uparrow$
$\gamma_0\gamma_1$	$-iS_\uparrow S_\downarrow - iS_\downarrow S_\uparrow - iP_\uparrow P_\downarrow - iP_\downarrow P_\uparrow$
$\gamma_1\gamma_5$	$-iS_\uparrow P_\downarrow - iS_\downarrow P_\uparrow + iP_\uparrow S_\downarrow + iP_\downarrow S_\uparrow$
$\gamma_0\gamma_1\gamma_5$	$-iS_\uparrow P_\downarrow - iS_\downarrow P_\uparrow - iP_\uparrow S_\downarrow - iP_\downarrow S_\uparrow$
γ_2	$-S_\uparrow S_\downarrow + S_\downarrow S_\uparrow + P_\uparrow P_\downarrow - P_\downarrow P_\uparrow$
$\gamma_0\gamma_2$	$+S_\uparrow S_\downarrow - S_\downarrow S_\uparrow + P_\uparrow P_\downarrow - P_\downarrow P_\uparrow$
$\gamma_2\gamma_5$	$+S_\uparrow P_\downarrow - S_\downarrow P_\uparrow - P_\uparrow S_\downarrow + P_\downarrow S_\uparrow$
$\gamma_0\gamma_2\gamma_5$	$+S_\uparrow P_\downarrow - S_\downarrow P_\uparrow + P_\uparrow S_\downarrow - P_\downarrow S_\uparrow$

Table 2.2: Relation between Γ in the (pseudo) physical basis and the static-light meson content

2.6 Symmetries and quantum numbers

As a first step, we have to look for symmetries of the $B\bar{B}$ system in order to label the different states by appropriate quantum numbers.

The $B\bar{B}$ system contains a light quark and a light antiquark, so isospin $I \in \{0, 1\}$ and its z-component $I_z \in \{+, -\}$ are quantum numbers.

The separation of the static quark and antiquark restricts rotational symmetry to rotations around the separation axis, i.e. the z-axis. Therefore, and since there are no interactions involving the spin of the static quark and antiquark, we can label the states by the z-component of the angular momentum of the light quarks $j_z \in \{-1, 0, +1\}$.

Regarding states with $j_z = 0$, reflecting along an axis orthogonal to the separation axis is also a symmetry (we choose without restriction of generality the x-axis). The corresponding quantum number $\mathscr{P}_x \in \{+, -\}$, referred to as "x-parity", can be used as a quantum number for all states, if we choose $|j_z|$ to label the $B\bar{B}$ states instead of j_z.

The separation of the static quark and antiquark also entails the fact that parity $\mathscr{P}$ alone is obviously no symmetry. However, combined with charge conjugation C it is, which means, $\mathscr{P} \circ C$ is an

appropriate quantum number to label the $B\bar{B}$ states.

Summing up, there are five different quantum numbers to label the $B\bar{B}$ states, i.e. I, I_z, $|j_z|$, $\mathscr{P}\circ C$ and $\mathscr{P}_x$.

To give an example, we show the calculation of some quantum numbers for a specific operator by using the following symmetry transformations. As introduced in section 2.2, $\{\psi, \bar{\psi}\}$ describe quark and antiquark fields of the (pseudo) physical basis and $\{\chi, \bar{\chi}\}$ quark and antiquark fields of the twisted basis. Regarding parity transformations in the twisted basis, we have to pay attention to the arising flavour exchange [6].

The used symmetry transformations are:

Parity $\mathscr{P}$:

$$\psi(\vec{r}) \xrightarrow{\mathscr{P}} \gamma_0 \psi(-\vec{r}) \implies \bar{\psi}(\vec{r}) \xrightarrow{\mathscr{P}} \bar{\psi}(-\vec{r})\gamma_0 \tag{2.33}$$

Twisted mass parity $\mathscr{P}^{(\mathrm{tm})}$:

$$\begin{aligned} \chi^{(u)}(\vec{r}) &\xrightarrow{\mathscr{P}^{(\mathrm{tm})}} \gamma_0 \chi^{(d)}(-\vec{r}) \implies \bar{\chi}^{(u)}(\vec{r}) \xrightarrow{\mathscr{P}^{(\mathrm{tm})}} \bar{\chi}^{(d)}(-\vec{r})\gamma_0 \\ \chi^{(d)}(\vec{r}) &\xrightarrow{\mathscr{P}^{(\mathrm{tm})}} \gamma_0 \chi^{(u)}(-\vec{r}) \implies \bar{\chi}^{(d)}(\vec{r}) \xrightarrow{\mathscr{P}^{(\mathrm{tm})}} \bar{\chi}^{(u)}(-\vec{r})\gamma_0 \end{aligned} \tag{2.34}$$

Charge conjugation C:

$$\psi(\vec{r}) \xrightarrow{\mathrm{C}} \gamma_0\gamma_2 \bar{\psi}^T(\vec{r}) \implies \bar{\psi}(\vec{r}) \xrightarrow{\mathrm{C}} -\psi^T(\vec{r})\gamma_2\gamma_0 \tag{2.35}$$

Parity combined with charge conjugation $\mathscr{P}\circ C$:

$$\psi(\vec{r}) \xrightarrow{\mathscr{P}\circ\mathrm{C}} \gamma_2 \bar{\psi}^T(-\vec{r}) \implies \bar{\psi}(\vec{r}) \xrightarrow{\mathscr{P}\circ\mathrm{C}} -\psi^T(-\vec{r})\gamma_2 \tag{2.36}$$

Twisted mass parity combined with charge conjugation $\mathscr{P}^{(\mathrm{tm})}\circ C$:

$$\begin{aligned} \chi^{(u)}(\vec{r}) &\xrightarrow{P^{(\mathrm{tm})}\circ C} \gamma_2 \bar{\chi}^{T(d)}(-\vec{r}) \implies \bar{\chi}^{(u)}(\vec{r}) \xrightarrow{P^{(\mathrm{tm})}\circ C} -\chi^{T(d)}(-\vec{r})\gamma_2 \\ \chi^{(d)}(\vec{r}) &\xrightarrow{P^{(\mathrm{tm})}\circ C} \gamma_2 \bar{\chi}^{T(u)}(-\vec{r}) \implies \bar{\chi}^{(d)}(\vec{r}) \xrightarrow{P^{(\mathrm{tm})}\circ C} -\chi^{T(u)}(-\vec{r})\gamma_2 \end{aligned} \tag{2.37}$$

The x-parity transformation $\mathscr{P}_x$ consists of an ordinary parity transformation $\mathscr{P}$ combined with a π-rotation around the x-axis. Therefore, we first consider rotations $\mathcal{R}_j(\vec{\alpha})$:

$$\psi(\vec{r}) \overset{\mathrm{R}_j(\vec{\alpha})}{\longrightarrow} \exp\left(-\frac{\alpha}{2}\gamma_0\gamma_j\gamma_5\right)\psi(\vec{r}\,') \implies \bar{\psi}(\vec{r}) \overset{\mathrm{R}_j(\vec{\alpha})}{\longrightarrow} \bar{\psi}(\vec{r}\,')\exp\left(-\frac{\alpha}{2}\gamma_5\gamma_j\gamma_0\right) \tag{2.38}$$

This yields for $j = 1$, i.e. rotations around the x-axis:

$$\begin{aligned}
\psi(x,y,z) &\overset{\mathrm{R}_1(\vec{\alpha})}{\longrightarrow} \exp\left(-\frac{\alpha}{2}\gamma_0\gamma_1\gamma_5\right)\psi(x,-y,-z) = \exp\left(+\frac{\alpha}{2}\gamma_2\gamma_3\right)\psi(x,-y,-z) \\
&= \left(\sum_{k=0}^{\infty}\frac{\left(\frac{\alpha}{2}\gamma_2\gamma_3\right)^k}{k!}\right)\psi(x,-y,-z) = \left[\sum_{m=0}^{\infty}\frac{\left(\frac{\alpha}{2}\gamma_2\gamma_3\right)^{2m}}{(2m)!} + \sum_{n=0}^{\infty}\frac{\left(\frac{\alpha}{2}\gamma_2\gamma_3\right)^{2n+1}}{(2n+1)!}\right]\psi(x,-y,-z) \\
&= \left[\sum_{m=0}^{\infty}(-1)^m\frac{\left(\frac{\alpha}{2}\right)^{2m}}{(2m)!} + \gamma_2\gamma_3\sum_{n=0}^{\infty}(-1)^n\frac{\left(\frac{\alpha}{2}\right)^{2n+1}}{(2n+1)!}\right]\psi(x,-y,-z) \\
&= \left[\cos\left(\frac{\alpha}{2}\right) + \gamma_2\gamma_3\sin\left(\frac{\alpha}{2}\right)\right]\psi(x,-y,-z) \overset{\alpha=\pi}{=} \gamma_2\gamma_3\,\psi(x,-y,-z)
\end{aligned} \tag{2.39}$$

x-parity $\mathscr{P}_x = \mathscr{P}\circ\mathcal{R}_1(\pi)$:

$$\psi(x,y,z) \overset{\mathscr{P}_x}{\longrightarrow} \gamma_1\gamma_5\psi(-x,y,z) \implies \bar{\psi}(x,y,z) \overset{\mathscr{P}_x}{\longrightarrow} \bar{\psi}(-x,y,z)\,\gamma_5\gamma_1 \tag{2.40}$$

Twisted mass x-parity $\mathscr{P}_x^{(\mathrm{tm})} = \mathscr{P}^{(\mathrm{tm})}\circ\mathcal{R}_1(\pi)$:

$$\begin{aligned}
\chi^{(u)}(\vec{r}) &\overset{\mathscr{P}_x^{(\mathrm{tm})}}{\longrightarrow} \gamma_1\gamma_5\chi^{(d)}(-x,y,z) \implies \bar{\chi}^{(u)}(\vec{r}) \overset{\mathscr{P}_x^{(\mathrm{tm})}}{\longrightarrow} \bar{\chi}^{(d)}(-x,y,z)\,\gamma_5\gamma_1 \\
\chi^{(d)}(\vec{r}) &\overset{\mathscr{P}_x^{(\mathrm{tm})}}{\longrightarrow} \gamma_1\gamma_5\chi^{(u)}(-x,y,z) \implies \bar{\chi}^{(d)}(\vec{r}) \overset{\mathscr{P}_x^{(\mathrm{tm})}}{\longrightarrow} \bar{\chi}^{(u)}(-x,y,z)\,\gamma_5\gamma_1
\end{aligned} \tag{2.41}$$

We are now able to compute the quantum numbers $\mathscr{P}\circ C$ and $\mathscr{P}_x$ both in the (pseudo) physical basis and in the twisted basis. Obviously, it is sufficient if we just regard the light quark and antiquark fields of (2.13). Looking at the structure of the spinor indices, we identify:

$$\Gamma_{AB}\,\psi_A(\vec{r}_1)\,\bar{\psi}_B(\vec{r}_2) \equiv \psi^T(\vec{r}_1)\,\Gamma\,\bar{\psi}^T(\vec{r}_2) \tag{2.42}$$

The preliminary considerations directly yield for the (pseudo) physical basis $\{\psi,\bar{\psi}\}$ and the twisted basis $\{\chi,\bar{\chi}\}$ (with $\vec{r}_1 = (0,0,+R/2)^T$ and $\vec{r}_2 = (0,0,-R/2)^T$):

$$\begin{aligned}
\psi^{T(m)}(\vec{r}_1)\,\Gamma\;\bar{\psi}^{T(n)}(\vec{r}_2) &\overset{\mathscr{P}\circ\mathrm{C}}{\longrightarrow} \left(\gamma_2\bar{\psi}^{T(m)}(\vec{r}_2)\right)^T\Gamma\left(-\psi^{T(n)}(\vec{r}_1)\gamma_2\right)^T = -\bar{\psi}^{(m)}(\vec{r}_2)\,\gamma_2\Gamma\gamma_2\,\psi^{(n)}(\vec{r}_1) \\
&= \psi^{T(n)}(\vec{r}_1)\,\gamma_2\Gamma^T\gamma_2\,\bar{\psi}^{T(m)}(\vec{r}_2) \implies \underline{u\bar{d} \leftrightarrow d\bar{u},\ \Gamma^T \to \Gamma,\ \Gamma \rightleftarrows \gamma_2}
\end{aligned} \tag{2.43}$$

$$\psi^{T(m)}(\vec{r}_1)\,\Gamma\,\bar{\psi}^{T(n)}(\vec{r}_2) \xrightarrow{\mathscr{P}_x} \left(\gamma_1\gamma_5\psi^{(m)}(\vec{r}_1)\right)^T \Gamma \left(\bar{\psi}^{(n)}(\vec{r}_2)\gamma_5\gamma_1\right)^T = \psi^{T(m)}(\vec{r}_1)\,\gamma_5\gamma_1^T\Gamma\gamma_1^T\gamma_5\,\bar{\psi}^{T(n)}(\vec{r}_2)$$
$$= \psi^{T(m)}(\vec{r}_1)\,\gamma_5\gamma_1\Gamma\gamma_1\gamma_5\,\bar{\psi}^{T(n)}(\vec{r}_2) \implies \underline{\Gamma \rightleftarrows \gamma_1,\ \Gamma \rightleftarrows \gamma_5}\ , \tag{2.44}$$

$$\chi^{T(m)}(\vec{r}_1)\,\Gamma\,\bar{\chi}^{T(n)}(\vec{r}_2) \xrightarrow{P^{(\mathrm{tm})}\circ C} \left(\gamma_2\bar{\chi}^{T(\tilde{m})}(\vec{r}_2)\right)^T \Gamma \left(-\chi^{T(\tilde{n})}(\vec{r}_1)\gamma_2\right)^T = -\bar{\chi}^{(\tilde{m})}(\vec{r}_2)\,\gamma_2\Gamma\gamma_2\,\chi^{(\tilde{n})}(\vec{r}_1)$$
$$= \chi^{T(\tilde{n})}(\vec{r}_1)\,\gamma_2\Gamma^T\gamma_2\,\bar{\chi}^{T(\tilde{m})}(\vec{r}_2) \implies \underline{u\bar{u} \leftrightarrow d\bar{d},\ \Gamma^T \to \Gamma,\ \Gamma \rightleftarrows \gamma_2} \tag{2.45}$$

$$\chi^{T(m)}(\vec{r}_1)\,\Gamma\,\bar{\chi}^{T(n)}(\vec{r}_2) \xrightarrow{\mathscr{P}_x^{(\mathrm{tm})}} \left(\gamma_1\gamma_5\chi^{(\tilde{m})}(\vec{r}_1)\right)^T \Gamma \left(\bar{\chi}^{(\tilde{n})}(\vec{r}_2)\gamma_5\gamma_1\right)^T = \chi^{T(\tilde{m})}(\vec{r}_1)\,\gamma_5\gamma_1^T\Gamma\gamma_1^T\gamma_5\,\bar{\chi}^{T(\tilde{n})}(\vec{r}_2)$$
$$= \chi^{T(\tilde{m})}(\vec{r}_1)\,\gamma_5\gamma_1\Gamma\gamma_1\gamma_5\,\bar{\chi}^{T(\tilde{n})}(\vec{r}_2) \implies \underline{u\bar{u} \leftrightarrow d\bar{d},\ u\bar{d} \leftrightarrow d\bar{u},\ \Gamma\rightleftarrows\gamma_1,\ \Gamma \rightleftarrows \gamma_5} \tag{2.46}$$

$\tilde{m}/\tilde{n}$ denotes a change of the flavour m/n, e.g. $m = u \Rightarrow \tilde{m} = d$. Furthermore, the notation of the underlined "rules", which describe how the signs in Table 2.3 and Table 2.4 come up, is the following: $\leftrightarrow$ describes the respective flavour exchange, $\Gamma \to \Gamma^T$ the transposition of the Γ matrix and $\Gamma \rightleftarrows \gamma_x$ a multiplication from both sides with γ_x.

$\psi^{(1)}\psi^{(2)}$		$= u\bar{u} + d\bar{d}$	$= u\bar{u} - d\bar{d}$	$\in \{u\bar{d}, d\bar{u}\}$
Γ	$\lvert j_z\rvert$	$\mathscr{P}\circ C, \mathscr{P}_x$	$\mathscr{P}\circ C, \mathscr{P}_x$	$\mathscr{P}_x$
γ_5	0	$-,-$	$-,-$	$-$
$\gamma_0\gamma_5$	0	$-,-$	$-,-$	$-$
1	0	$+,+$	$+,+$	$+$
γ_0	0	$-,+$	$-,+$	$+$
γ_3	0	$+,+$	$+,+$	$+$
$\gamma_0\gamma_3$	0	$+,+$	$+,+$	$+$
$\gamma_3\gamma_5$	0	$+,-$	$+,-$	$-$
$\gamma_0\gamma_3\gamma_5$	0	$-,-$	$-,-$	$-$
γ_1	1	$+,-$	$+,-$	$-$
γ_2	1	$+,+$	$+,+$	$+$
$\gamma_0\gamma_1$	1	$+,-$	$+,-$	$-$
$\gamma_0\gamma_2$	1	$+,+$	$+,+$	$+$
$\gamma_1\gamma_5$	1	$+,+$	$+,+$	$+$
$\gamma_2\gamma_5$	1	$+,-$	$+,-$	$-$
$\gamma_0\gamma_1\gamma_5$	1	$-,+$	$-,+$	$+$
$\gamma_0\gamma_2\gamma_5$	1	$-,-$	$-,-$	$-$

Table 2.3: Quantum numbers in the (pseudo) physical basis

$\chi^{(1)}\chi^{(2)}$		$= u\bar{u} + d\bar{d}$	$= u\bar{d} - d\bar{u}$	$\in \{u\bar{d}, d\bar{u}\}$
Γ	$\lvert j_z\rvert$	$\mathscr{P}^{(\mathrm{tm})} \circ C, \mathscr{P}_x^{(\mathrm{tm})}$	$\mathscr{P}^{(\mathrm{tm})} \circ C, \mathscr{P}_x^{(\mathrm{tm})}$	$\mathscr{P}^{(\mathrm{tm})} \circ C$
γ_5	0	$-, -$	$+, +$	$-$
$\gamma_0\gamma_5$	0	$-, -$	$+, +$	$-$
1	0	$+, +$	$-, -$	$+$
γ_0	0	$-, +$	$+, -$	$-$
γ_3	0	$+, +$	$-, -$	$+$
$\gamma_0\gamma_3$	0	$+, +$	$-, -$	$+$
$\gamma_3\gamma_5$	0	$+, -$	$-, +$	$+$
$\gamma_0\gamma_3\gamma_5$	0	$-, -$	$+, +$	$-$
γ_1	1	$+, -$	$-, +$	$+$
γ_2	1	$+, +$	$-, -$	$+$
$\gamma_0\gamma_1$	1	$+, -$	$-, +$	$+$
$\gamma_0\gamma_2$	1	$+, +$	$-, -$	$+$
$\gamma_1\gamma_5$	1	$+, +$	$-, -$	$+$
$\gamma_2\gamma_5$	1	$+, -$	$-, +$	$+$
$\gamma_0\gamma_1\gamma_5$	1	$-, +$	$+, -$	$-$
$\gamma_0\gamma_2\gamma_5$	1	$-, -$	$+, +$	$-$

Table 2.4: Quantum numbers in the twisted basis

These results combined with those of section 2.5 concerning the meson content are collected in Table 2.5 for the flavour combinations $u\bar{u} \pm d\bar{d}$ and in Table 2.6 for the flavour combinations $u\bar{d}/d\bar{u}$.[4]

The different states are organised in multiplets A-L in the (pseudo) physical basis and in sections *a-l* in the twisted basis.

The signs in Table 2.5, which are enclosed in brackets above several γ matrices describe the corresponding signs between $u\bar{u}$ and $d\bar{d}$, i.e. $u\bar{u} + d\bar{d}$ or $u\bar{u} - d\bar{d}$.

In Table 2.6 all upper signs correspond to $u\bar{d}$ and all lower signs to $d\bar{u}$. For instance, to get the quantum numbers shown in the first line in the twisted basis we have to consider the flavour combination $u\bar{d}$ with $\Gamma = \gamma_5 + i\gamma_0$ or $d\bar{u}$ with $\Gamma = \gamma_5 - i\gamma_0$. This splitting is due to the different used bases (cf. section 2.2).

4 The corresponding tables for BB systems are presented in Appendix A.

$\Gamma^{(u\bar{u}\pm d\bar{d})}$ tb	$\mathscr{P}^{(\mathrm{tm})} \circ C, \mathscr{P}_x^{(\mathrm{tm})}$	sec.	$\Gamma^{(u\bar{u}\pm d\bar{d})}$ ppb	$\mathscr{P} \circ C, \mathscr{P}_x$	type	mult.
$j_z = 0,\ I = 0$						
$i^{(-)} - \gamma_0\gamma_5^{(+)}$	$-,\ -$	a	$(+\gamma_5 - \gamma_0\gamma_5)^{(+)}$	$-,\ -$	SS	A
$\gamma_0\gamma_3^{(-)}$	$-,\ -$	a	$-i\gamma_0\gamma_3\gamma_5^{(+)}$	$-,\ -$	SP_-	A
$i^{(-)} + \gamma_0\gamma_5^{(+)}$	$-,\ -$	a	$(+\gamma_5 + \gamma_0\gamma_5)^{(+)}$	$-,\ -$	P_-P_-	A
$\gamma_3^{(+)} - i\gamma_0\gamma_3\gamma_5^{(-)}$	$+,\ +$	b	$(+\gamma_3 - \gamma_0\gamma_3)^{(+)}$	$+,\ +$	SS	B
$\gamma_5^{(-)}$	$+,\ +$	b	$-i^{(+)}$	$+,\ +$	SP_-	B
$\gamma_3^{(+)} + i\gamma_0\gamma_3\gamma_5^{(-)}$	$+,\ +$	b	$(+\gamma_3 + \gamma_0\gamma_3)^{(+)}$	$+,\ +$	P_-P_-	B
$\gamma_3\gamma_5^{(+)}$	$+,\ -$	c	$+\gamma_3\gamma_5^{(+)}$	$+,\ -$	SP_-	C
$\gamma_0^{(+)}$	$-,\ +$	d	$+\gamma_0^{(+)}$	$-,\ +$	SP_-	D
$j_z = 0,\ I = 1,\ I_z = 0$						
$i^{(+)} - \gamma_0\gamma_5^{(-)}$	$+,\ +$	b	$(+\gamma_5 - \gamma_0\gamma_5)^{(-)}$	$-,\ -$	SS	E
$\gamma_0\gamma_3^{(+)}$	$+,\ +$	b	$-i\gamma_0\gamma_3\gamma_5^{(-)}$	$-,\ -$	SP_-	E
$i^{(+)} + \gamma_0\gamma_5^{(-)}$	$+,\ +$	b	$(+\gamma_5 + \gamma_0\gamma_5)^{(-)}$	$-,\ -$	P_-P_-	E
$\gamma_3^{(-)} - i\gamma_0\gamma_3\gamma_5^{(+)}$	$-,\ -$	a	$(+\gamma_3 - \gamma_0\gamma_3)^{(-)}$	$+,\ +$	SS	F
$\gamma_5^{(+)}$	$-,\ -$	a	$-i^{(-)}$	$+,\ +$	SP_-	F
$\gamma_3^{(-)} + i\gamma_0\gamma_3\gamma_5^{(+)}$	$-,\ -$	a	$(+\gamma_3 + \gamma_0\gamma_3)^{(-)}$	$+,\ +$	P_-P_-	F
$\gamma_3\gamma_5^{(-)}$	$-,\ +$	d	$+\gamma_3\gamma_5^{(-)}$	$+,\ -$	SP_-	G
$\gamma_0^{(-)}$	$+,\ -$	c	$+\gamma_0^{(-)}$	$-,\ +$	SP_-	H
$j_z = 1,\ I = 0$						
$\gamma_{1/2}^{(+)} - i\gamma_0\gamma_{1/2}\gamma_5^{(-)}$	$+,\ -/+$	e/f	$(+\gamma_{1/2} - \gamma_0\gamma_{1/2})^{(+)}$	$+,\ -/+$	SS	I
$\gamma_{2/1}\gamma_5^{(+)}$	$+,\ -/+$	e/f	$+\gamma_{2/1}\gamma_5^{(+)}$	$+,\ -/+$	SP_-	I
$\gamma_{1/2}^{(+)} + i\gamma_0\gamma_{1/2}\gamma_5^{(-)}$	$+,\ -/+$	e/f	$(+\gamma_{1/2} + \gamma_0\gamma_{1/2})^{(+)}$	$+,\ -/+$	P_-P_-	I
$\gamma_0\gamma_{1/2}^{(-)}$	$-,\ -/+$	g/h	$-i\gamma_0\gamma_{1/2}\gamma_5^{(+)}$	$-,\ +/-$	SP_-	J
$j_z = 1,\ I = 1,\ I_z = 0$						
$\gamma_{1/2}^{(-)} - i\gamma_0\gamma_{1/2}\gamma_5^{(+)}$	$-,\ +/-$	h/g	$(+\gamma_{1/2} - \gamma_0\gamma_{1/2})^{(-)}$	$+,\ -/+$	SS	K
$\gamma_{2/1}\gamma_5^{(-)}$	$-,\ +/-$	h/g	$+\gamma_{2/1}\gamma_5^{(-)}$	$+,\ -/+$	SP_-	K
$\gamma_{1/2}^{(-)} + i\gamma_0\gamma_{1/2}\gamma_5^{(+)}$	$-,\ +/-$	h/g	$(+\gamma_{1/2} + \gamma_0\gamma_{1/2})^{(-)}$	$+,\ -/+$	P_-P_-	K
$\gamma_0\gamma_{1/2}^{(+)}$	$+,\ +/-$	f/e	$-i\gamma_0\gamma_{1/2}\gamma_5^{(-)}$	$-,\ +/-$	SP_-	L

Table 2.5: Twisted and physical quantum numbers for $u\bar{u} \pm d\bar{d}$

$\Gamma^{\binom{u\bar{d}}{d\bar{u}}}$ tb	$\mathscr{P}^{(\mathrm{tm})}\circ C$	sec.	$\Gamma^{\binom{u\bar{d}}{d\bar{u}}}$ ppb	$\mathscr{P}_x$	type	mult.
$j_z = 0,\ I = 1,\ I_z = \pm 1$						
$\gamma_5 \pm i\gamma_0$	$-$	i	$+\gamma_5 - \gamma_0\gamma_5$	$-$	SS	E
$\gamma_0\gamma_3\gamma_5$	$-$	i	$+\gamma_0\gamma_3\gamma_5$	$-$	SP_-	E
$\gamma_5 \mp i\gamma_0$	$-$	i	$+\gamma_5 + \gamma_0\gamma_5$	$-$	P_-P_-	E
$\gamma_0\gamma_3 \pm i\gamma_3\gamma_5$	$+$	j	$+\gamma_0\gamma_3 - \gamma_3$	$+$	SS	F
1	$+$	j	$+1$	$+$	SP_-	F
$\gamma_0\gamma_3 \mp i\gamma_3\gamma_5$	$+$	j	$+\gamma_0\gamma_3 + \gamma_3$	$+$	P_-P_-	F
γ_3	$+$	j	$\pm i\gamma_3\gamma_5$	$-$	SP_-	G
$\gamma_0\gamma_5$	$-$	i	$\pm i\gamma_0$	$+$	SP_-	H
$j_z = 1,\ I = 1,\ I_z = \pm 1$						
$\gamma_0\gamma_{1/2} \pm i\gamma_{1/2}\gamma_5$	$+/+$	k	$+\gamma_0\gamma_{1/2} - \gamma_{1/2}$	$-/+$	SS	I
$\gamma_{2/1}$	$+/+$	k	$\pm i\gamma_{2/1}\gamma_5$	$-/+$	SP_-	I
$\gamma_0\gamma_{1/2} \mp i\gamma_{1/2}\gamma_5$	$+/+$	k	$+\gamma_0\gamma_{1/2} + \gamma_{1/2}$	$-/+$	P_-P_-	I
$\gamma_0\gamma_{1/2}\gamma_5$	$-/-$	l	$+\gamma_0\gamma_{1/2}\gamma_5$	$+/-$	SP_-	J

Table 2.6: Twisted and physical quantum numbers for $u\bar{d}$ and $d\bar{u}$

2.7 Diagrams

For the numerical calculations of the $B\bar{B}$ systems it is helpful to look at the possible diagrams of the different correlation functions. In these diagrams the separation r along the z-axis is represented in horizontal direction and the time t is developing in vertical direction. Unfilled circles describe quarks whereas filled circles are meant to be antiquarks. The lines represent the propagators and as before, the static quarks and antiquarks are labelled by Q and $\bar{Q}$, respectively.

Since static quarks have fixed positions and therefore only propagate in time, they can just form vertical lines. In contrast to that, the light quarks are not located at a fixed point and thus the structure of the correlation function at time t can differ from that at time 0.

An example for such an "exchange" of the light quarks within the structure of the correlation function, a so called cross diagram, can be seen in Figure 2.1(b), as well as a so called two meson diagram (a).

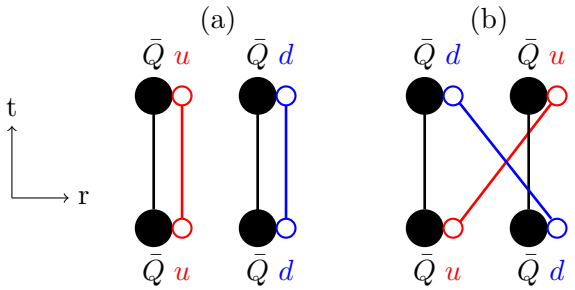

Figure 2.1: Two meson diagram (a) and cross diagram (b)

2.7.1 BB systems

The possible diagrams regarding a BB system are the two shown in Figure 2.1. Figure 2.2 shows the possible diagrams for isospin $I = 0$ and Figure 2.3 those for $I = 1$ depending on the different flavour combinations.

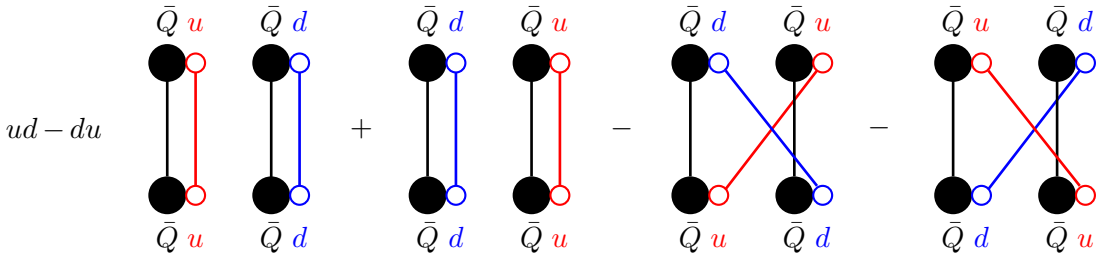

Figure 2.2: Diagrams for BB systems ($I = 0$)

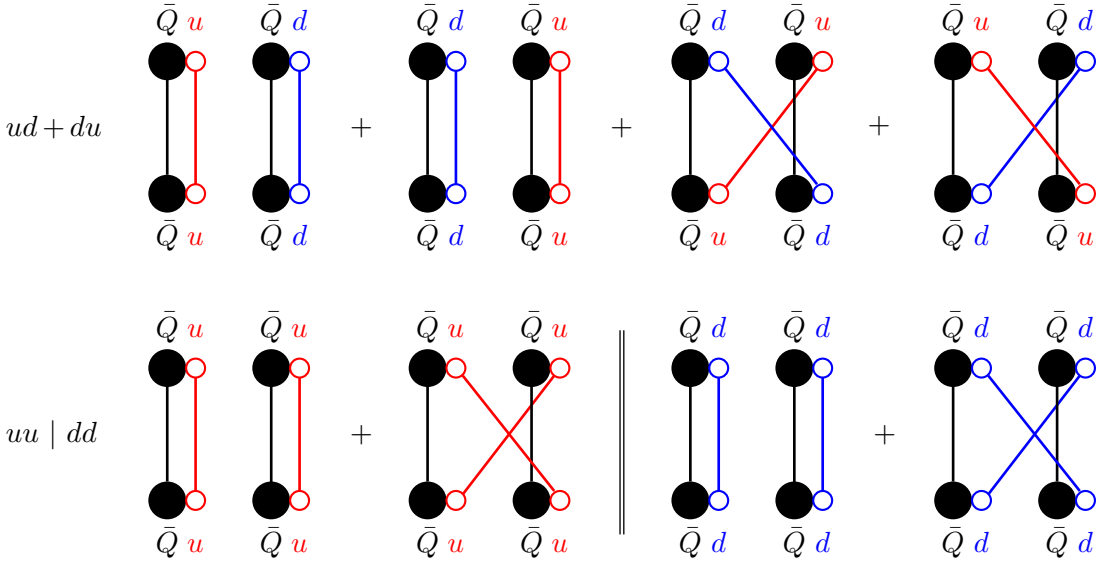

Figure 2.3: Diagrams for BB systems ($I = 1$)

As can be seen, regardless of the choice of the flavour combination, both diagrams, i.e. the two meson diagram and the cross diagram, are possible and have to be computed.

2.7.2 $B\bar{B}$ systems

Obviously, for $B\bar{B}$ systems the cross diagram is not allowed. However, there are new diagrams, the so called box diagrams, which are shown in Figure 2.4.

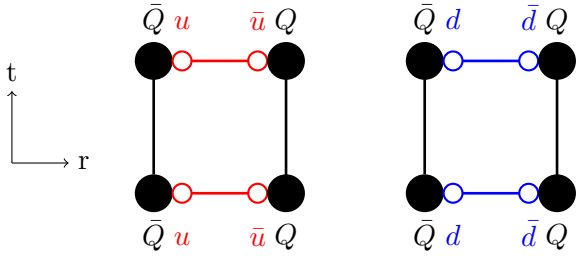

Figure 2.4: Box diagrams

These diagrams can be interpreted as the annihilation of the corresponding light quark and antiquark.

Figure 2.5 and Figure 2.6 show the possible diagrams for $B\bar{B}$ systems with $I = 0$ and $I = 1$, respectively.

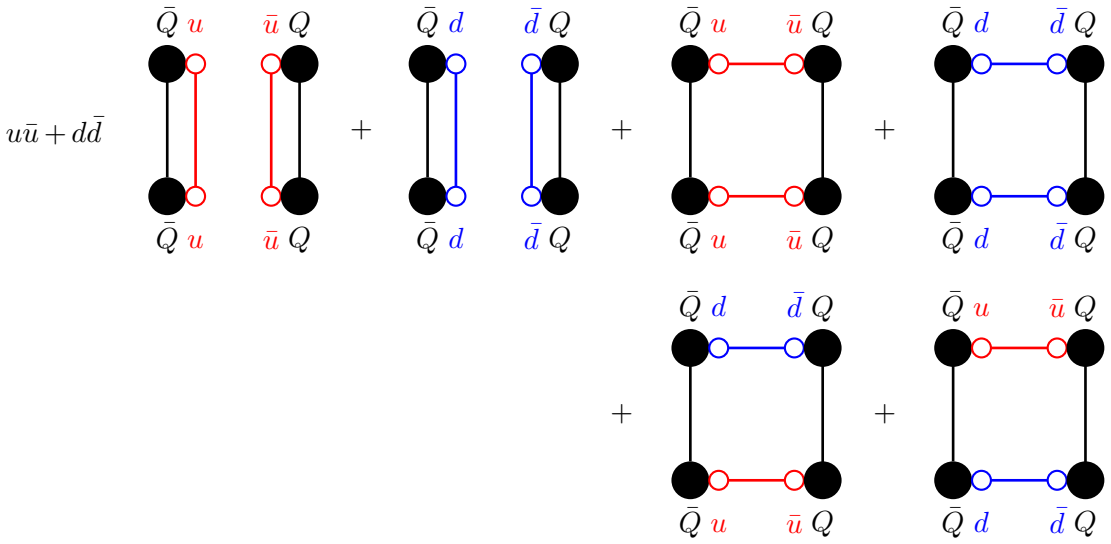

Figure 2.5: Diagrams for $B\bar{B}$ systems ($I = 0$)

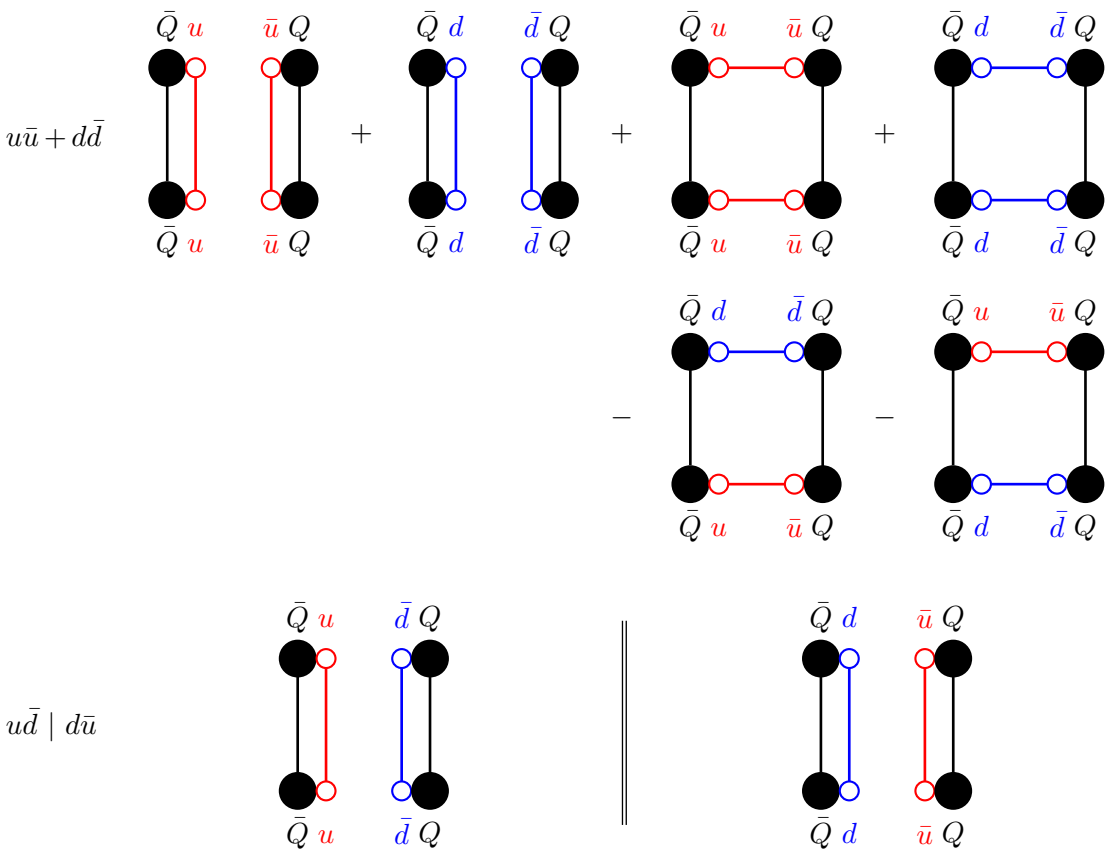

Figure 2.6: Diagrams for $B\bar{B}$ systems ($I = 1$)

A wide difference to the diagrams of BB systems is that for different light quark flavours only the two meson diagram has to be considered. This means that by computing the two meson diagram half of the potentials, i.e. all those with $I = 1$, can be calculated.[5] Therefore and since it was easier to implement into the initial code, we focused as a starting point on this type of diagram.

5 The correlation functions of $u\bar{d}$ and $d\bar{u}$ are related to those of $u\bar{u} - u\bar{u}$ via isospin transformations.

Chapter 3

Technical realisation

3.1 Computation of the light quark propagator

Unlink the static quark propagators, which are based on the link variables, the computation of the light quark propagators is very costly concerning computation time. Nevertheless, there are different possibilities to compute light quark propagators, while in this work only stochastic timeslice sources were used. This section is meant to show the basics of this method. Fore more information we refer to [13, 14].

A stochastic timeslice source located at $\tilde{t}$ is defined by

$$\xi[\tilde{t}]^a_A(x) = \delta(x_0 - \tilde{t}) \left(\pm\frac{1}{\sqrt{2}} \pm \frac{1}{\sqrt{2}}\, i \right), \tag{3.1}$$

where the two "$\pm$"-signs are chosen independently, as well as the different entries on the timeslice $\tilde{t}$. In our calculations, we used $N = 6$ different timeslice sources both for the u quark propagator and for the d quark propagator at each timeslice $\tilde{t}$. They fulfil:

$$\begin{aligned} \frac{1}{N} \sum_{n=1}^{N} \xi[n,\tilde{t}]^a_A(x) \Big(\xi[n,\tilde{t}]^b_B(y) \Big)^* = \delta^{ab}\delta_{AB}\delta(x_0 - \tilde{t})\delta(y_0 - \tilde{t})\delta(\vec{x} - \vec{y}) \\ + \ \mathrm{O}(1/\sqrt{N}) \text{ off-diagonal noise} \end{aligned} \tag{3.2}$$

To obtain the light quark propagator D^{-1}, we have to solve the following N linear systems for given timeslice sources ξ:

$$D^{ab}_{AB}(x;y)\, \phi[n,\tilde{t}]^b_B(y) = \xi[n,\tilde{t}]^a_A(x)\,, \quad n = 1, \ldots, N \tag{3.3}$$

ϕ is the so called sink and D the Dirac matrix. This yields:

$$\begin{aligned}
&\frac{1}{N}\sum_{n=1}^{N}\phi[n,\tilde{t}]^a_A(x)\Big(\xi[n,\tilde{t}]^b_B(y)\Big)^* \\
&= (D^{-1})^{ac}_{AC}(x;z)\,\frac{1}{N}\sum_{n=1}^{N}\xi[n,\tilde{t}]^c_C(z)\Big(\xi[n,\tilde{t}]^b_B(y)\Big)^* \\
&= (D^{-1})^{ab}_{AB}(x;y)\,\delta(y_0-\tilde{t}) + \mathrm{O}(1/\sqrt{N})\ \text{off-diagonal noise}
\end{aligned} \tag{3.4}$$

Hence, after generating the timeslice sources ξ and solving the linear equations (3.3), which yields the sinks ϕ, we have an expression for the light quark propagator D^{-1}.

3.2 Relation between the contractions and the correlation functions

We are now able to compute the correlation functions, which are essential for the computation of the potentials. In the following, we will distinguish between physical correlation functions C, introduced in (2.9), and a more fundamental version of these correlation functions, which we will call contractions C. These contractions C are easier to implement and can be related to the physical correlation functions C.

Here is an example for the contraction C of the two meson diagram introduced in section 2.7:

$$\begin{aligned}
&\mathsf{C}^{2\mathrm{meson}}(r,t) \\
&\quad= \Gamma(0)_{AB}\ \Gamma(t)_{CD} \\
&\quad\Big\langle\Big[(\phi^{a,(\alpha)}_C(0,t))^*\ U^{ab}(0,t;0,0)\ \xi^{b,(\alpha)}_A(0,0)\Big]\Big[(\xi^{c,(\beta)}_B(r,0))^*\ U^{cd}(r,0;r,t)\ \phi^{d,(\beta)}_D(r,t)\Big]\Big\rangle \\
&\quad= \Big((\Gamma(0)_{AB})^*\ (\Gamma(t)_{CD})^* \\
&\quad\Big\langle\Big[U^{ba}(0,0;0,t)\ \phi^{a,(\alpha)}_C(0,t)\ (\xi^{b,(\alpha)}_A(0,0))^*\Big]\Big[U^{dc}(r,t;r,0)\ (\phi^{d,(\beta)}_D(r,t)\ (\xi^{c,(\beta)}_B(r,0))^*)^*\Big]\Big\rangle\Big)^* \\
&\quad= \Big((\Gamma(0)_{AB})^*\ (\Gamma(t)_{CD})^* \\
&\quad\Big\langle\Big[U^{ba}(0,0;0,t)\,(D^{-1})^{ab,(\alpha)}_{CA}(0,t;0,0)\Big]\Big[U^{dc}(r,t;r,0)\,((D^{-1})^{dc,(\beta)}_{DB}(r,t;r,0))^*\Big]\Big\rangle\Big)^* \\
&\quad= \Big((\Gamma(0)_{AB})^*\ (\Gamma(t)_{CD})^* \\
&\quad\Big\langle\Big[U^{ba}(0,0;0,t)\,(D^{-1})^{ab,(\alpha)}_{CA}(0,t;0,0)\Big]\Big[U^{dc}(r,t;r,0)\,((\gamma_5(D^{-1})^\dagger\gamma_5)^{dc,(\tilde{\beta})}_{DB}(r,t;r,0))^*\Big]\Big\rangle\Big)^* = ...
\end{aligned}$$

$$
\begin{aligned}
... \;=\; & \Big((\Gamma(0)_{AB})^* \; (\Gamma^T(t)_{DC})^* \\
& \Big\langle \Big[U^{ba}(0,0;0,t) \, (D^{-1})^{ab,(\alpha)}_{CA}(0,t;0,0) \Big] \Big[U^{dc}(r,t;r,0) \, (\gamma_5 (D^{-1}) \gamma_5)^{cd,(\tilde{\beta})}_{BD}(r,0;r,t) \Big] \Big\rangle \Big)^* \\
=\; & \Big(((\Gamma(0)\gamma_5)_{AB})^* \; ((\gamma_5 \Gamma^T(t))_{DC} \Big)^* \\
& \Big\langle \Big[U^{ba}(0,0;0,t) \, (D^{-1})^{ab,(\alpha)}_{CA}(0,t;0,0) \Big] \Big[U^{dc}(r,t;r,0) \, (D^{-1})^{cd,(\tilde{\beta})}_{BD}(r,0;r,t) \Big] \Big\rangle \Big)^* \\
=\; & \Big(((\Gamma(0)\gamma_5)_{AB})^* \; ((\gamma_5 \Gamma^T(t))_{DC} \Big)^* \\
& \Big\langle \mathrm{Tr}_{\mathrm{col}} \Big[U(0,0;0,t) \, (D^{-1})^{(\alpha)}_{CA}(0,t;0,0) \Big] \, \mathrm{Tr}_{\mathrm{col}} \Big[U(r,t;r,0) \, (D^{-1})^{(\tilde{\beta})}_{BD}(r,0;r,t) \Big] \Big\rangle \Big)^*
\end{aligned} \tag{3.5}
$$

As in subsection 2.3.3, $\Gamma(t)$ denotes the Γ matrix within the operator $\mathcal{O}(t)$ and $\Gamma(0)$ the Γ matrix within the operator $\mathcal{O}(0)$. There is of course no time dependence of the Γ matrices.

These contractions were computed for any of the 16×16 combinations of the two involved Γ matrices, for each spatial direction x, y and z, both for positive and negative time direction, and for the four different flavour combinations.

The comparison of (3.5) and (2.21) yields the relation between the computed contractions C and the physical correlation functions C we are looking for:

- We have to use the computed contractions in negative time direction.
- $C^{2\mathrm{meson}}(r,t) = -2(\mathsf{C}^{2\mathrm{meson}}(r,t))^*$
- The Γ matrices are related by:
  - $\Gamma(0)_{\mathrm{contr.\,code}} = \gamma_0 \Gamma(t)_{\mathrm{cor.\,func.}} \gamma_0 \gamma_5$
  - $\Gamma(t)_{\mathrm{contr.\,code}} = (\Gamma(0)_{\mathrm{cor.\,func.}})^* \gamma_5$
- The second light quark flavour β exchanges due to the used twisted mass γ_5-hermiticity. Since we use the negative time direction, this is the flavour of the light quark and not the light antiquark, which means $u\bar{u} \leftrightarrow d\bar{u}$ and $u\bar{d} \leftrightarrow d\bar{d}$.

3.3 Symmetry checks and symmetry averaging

Symmetry checks are a very useful tool to affirm the computed results of the contractions. One performs a symmetry transformation and creates rules to identify the contraction pairs, which are connected via this symmetry transformation.

The available symmetries are:

- Twisted mass time reversal
- Twisted mass parity
- Twisted mass γ_5-hermiticity
- Charge conjugation
- Cubic $\frac{\pi}{2}$-rotations around all spacial axes
- Cubic π-rotations around the x- and y-axis

In the following, we will show the procedure for the twisted mass time reversal in detail.

Performing a twisted mass time reversal transformation results in:

$$\begin{aligned}
&(\Gamma(0)\gamma_5)^*_{AB}(\gamma_5\Gamma^T(t))^*_{DC}\,\psi^\alpha_C(0,t)\,\bar{\psi}^\alpha_A(0,0)\,\psi^\beta_B(r,0)\,\bar{\psi}^\beta_D(r,t)\\
&\quad\xrightarrow{\mathrm{T^{(tm)}}}(\Gamma(0)\gamma_5)^*_{AB}(\gamma_5\Gamma^T(t))^*_{DC}\\
&\qquad(\gamma_0\gamma_5)_{CV}\,\psi^{\tilde{\alpha}}_V(0,-t)\,\bar{\psi}^{\tilde{\alpha}}_W(0,0)\,(\gamma_5\gamma_0)_{WA}\,(\gamma_0\gamma_5)_{BX}\,\psi^{\tilde{\beta}}_X(r,0)\,\bar{\psi}^{\tilde{\beta}}_Y(r,-t)\,(\gamma_5\gamma_0)_{YD}\\
&\quad=(\gamma_5\gamma_0\Gamma(0)\gamma_5\gamma_0\gamma_5)^*_{WX}(\gamma_5\gamma_0\gamma_5\Gamma^T(t)\gamma_0\gamma_5)^*_{YV}\,\psi^{\tilde{\alpha}}_V(0,-t)\,\bar{\psi}^{\tilde{\alpha}}_W(0,0)\,\psi^{\tilde{\beta}}_X(r,0)\,\bar{\psi}^{\tilde{\beta}}_Y(r,-t)\\
&\quad=(\gamma_5\gamma_0\Gamma(0)\gamma_0)^*_{AB}(\gamma_0\Gamma^T(t)\gamma_0\gamma_5)^*_{DC}\,\psi^{\tilde{\alpha}}_C(0,-t)\,\bar{\psi}^{\tilde{\alpha}}_A(0,0)\,\psi^{\tilde{\beta}}_B(r,0)\,\bar{\psi}^{\tilde{\beta}}_D(r,-t) \qquad (3.6)
\end{aligned}$$

This yields the following rules:

- We have to relate the contractions computed in positive time direction with those computed in negative time direction.
- Both flavours exchange, i.e. $u\bar{d} \leftrightarrow d\bar{u}$ and $u\bar{u} \leftrightarrow d\bar{d}$.
- The Γ matrices have to be transformed in the following way:
  - $(\Gamma(0)\gamma_5)^* \rightarrow (\gamma_5\gamma_0\Gamma(0)\gamma_0)^*$
  - $\left(\gamma_5\Gamma^T(t)\right)^* \rightarrow \left(\gamma_0\Gamma(t)^T\gamma_0\gamma_5\right)^*$

  $\Longrightarrow$ We get an extra minus sign, if $\Gamma(0)$ or $\Gamma(t) \in \{\gamma_5, \gamma_0, \gamma_0\gamma_3, \gamma_3\gamma_5, \gamma_0\gamma_1, \gamma_1\gamma_5, \gamma_0\gamma_2, \gamma_2\gamma_5\}$.

Figure 3.1 shows four examples for these general rules[1]. In each case we check the contractions computed in positive time direction and light quark flavour combination $d\bar{u}$ (green/dark blue) against those, which were computed in negative time direction with flavour combination $u\bar{d}$ (pink/light blue).

1 The simulation setup, including the ensemble E17.32, which was used in Figure 3.1, will be discussed in section 4.1.

According to the above mentioned rules, the absolute value of these contractions should be equal up to statistical fluctuations. Depending on the choice for $\Gamma(0)$ and $\Gamma(t)$ they have different signs.

Obviously, choosing $\Gamma(0) = \Gamma(t)$ should yield real and positive definite contractions C. A corresponding example is given in Figure 3.1 (a), where $\Gamma(0) = \Gamma(t) = 1$ is chosen.

However, contractions with $\Gamma(0) \neq \Gamma(t)$ can either be real or imaginary and do no longer have to be positive definite. In (b) we replaced one of the identity matrices by γ_0, which is one of the matrices that cause an extra minus sign.

Figure 3.1 (c) and (d) show purely imaginary contractions, each for $\Gamma(t) = \gamma_0\gamma_5$. As expected, combined with $\Gamma(0) = 1$ both contractions have the same sign and the choice $\Gamma(0) = \gamma_0$ yields different signs.

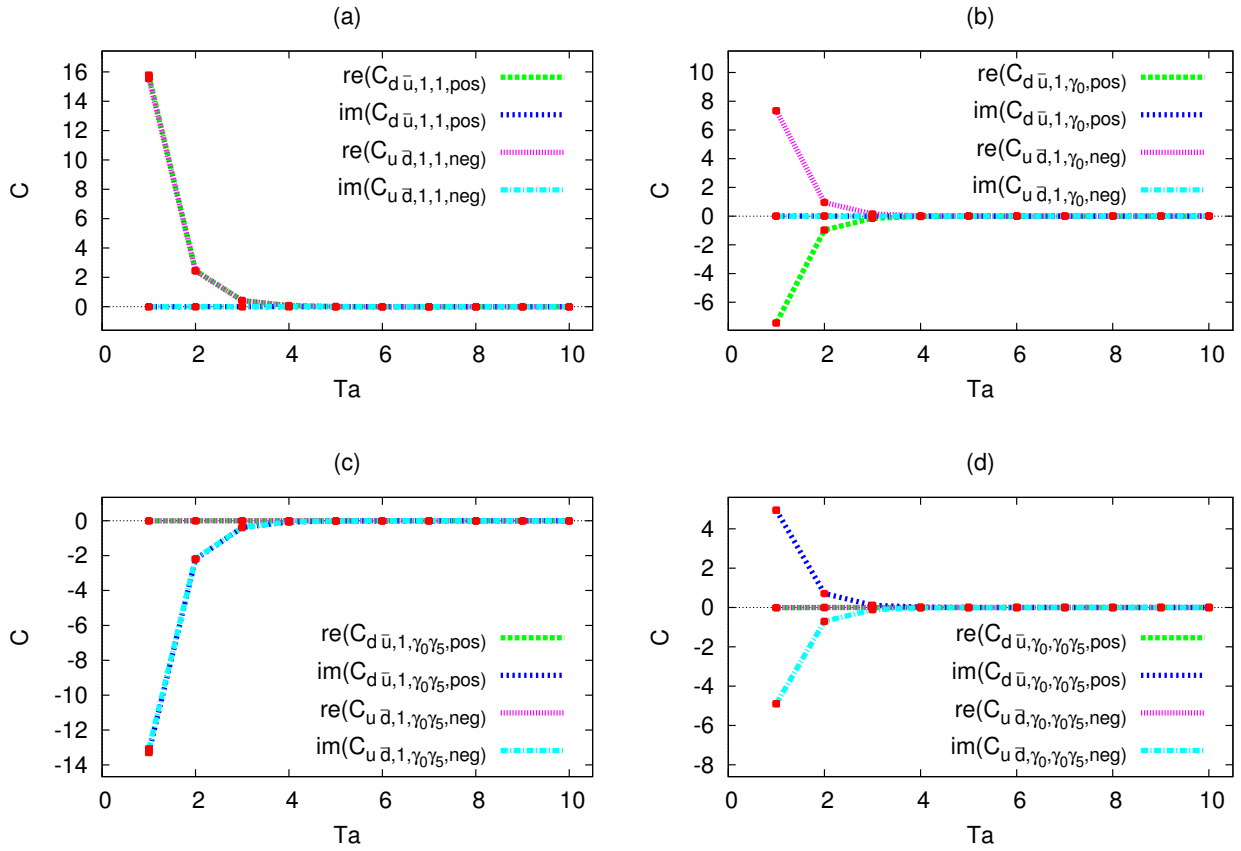

Figure 3.1: Comparison of real and imaginary part of each two contractions $\mathsf{C}_{\text{flavour combination, }\Gamma(0),\,\Gamma(t),\text{ time direction}}$ at $R = 4a$ with regard to twisted mass time reversal (lattice units)

Any used contraction has been checked for each of the nine above mentioned symmetries, which means that several thousand plots like the examples shown in Figure 3.1 were generated and checked. Afterwards we averaged over the contractions that were related by one or more of these symmetries.

This approach not only decreases the statistical errors, but also supports the credibility of the numerical results in a large amount.

Chapter 4

Numerical results

4.1 Lattice setup

In this work two different ensembles were used. In order to compare the results to those of the BB potentials in [3–5], we started our computations with a very similar lattice setup, i.e. same lattice extension and comparable lattice spacing a.[1] The main difference is that we used $N_f = 2 + 1 + 1$ dynamical quark flavours instead of $N_f = 2$. Since s and c sea quarks are considered, this yields a more realistic simulation, i.e. the systematic errors are reduced.

For the computations of the potentials with s and c quarks we then used a finer lattice to get a higher resolution at short distances. Otherwise, especially considering c quarks, there would have been too few non-vanishing values to get a good fit for the potentials. An ensemble with the required fine lattice spacing was not existent for $N_f = 2 + 1 + 1$ and therefore we were in this case restricted to $N_f = 2$.

The two used ensembles with their relevant parameters are shown in Table 4.1.

Ensemble	N_f	β	$(L/a)^3 \times (T/a)$	κ	$a\mu_l$	$a\mu_\sigma$	$a\mu_\delta$
A40.24	2+1+1	1.9	$24^3 \times 48$	0.16327	0.004	0.15	0.19
E17.32	2	4.35	$32^3 \times 64$	0.15174	0.00175	-	-

Table 4.1: Parameters of the used ensembles

L and T correspond to the lattice extensions in space and time, respectively, while μ_l, μ_σ and μ_δ are

1 All computations were performed in units of the lattice spacing a. For a better understanding we present some results in physical units (fm, MeV). For the transformation we used $a = 0.086\,\text{fm}$ for ensemble A40.24 and $a = 0.042\,\text{fm}$ for ensemble E17.32 (cf. [15, 16] for more information about the ensembles).

the twisted mass parameters of the sea quarks. Furthermore, the hopping parameter κ is connected to the untwisted quark mass m_q, introduced in (2.2), in the following way [6]:

$$\kappa = \frac{1}{2(am_q + 4)} \tag{4.1}$$

For each computed potential we used about 100 gauge field configurations and the twisted quark mass values μ_q (cf. (2.2) and (2.3)) listed in Table 4.2.

flavour	A40.24	E17.32
μ_s	-	0.0115
μ_c	0.27678	0.1320

Table 4.2: Twisted quark mass values μ_q used for the different ensembles

4.2 $\bar{Q}\bar{Q}$ potentials

This section shows the numerical results of potentials between two mesons in different channels. The mesons are both built up from a static antiquark and a quark of finite mass. We will consider s and c quarks and compare the potentials with existing results for light quarks.

To improve the signal quality we applied APE and Gaussian smearing. In addition, all computations are both done with the HYP2 static action, which yields an enhanced signal to noise ratio, and without using HYP2 smeared links, just as done in [3]. This is because ultraviolet fluctuations are relevant especially for small separations (i.e. $R \lesssim 2a$) and are filtered out by using the HYP2 static action. For more information concerning these smearing techniques cf. [17].

To be able to unite the two results, the potentials have to be normalised. Since we know the asymptotic behaviour of the potentials out of their static-light meson content (cf. section 2.5), we computed the corresponding meson masses, also with and without HYP2 smeared links, and used them for normalisation.

In order to plug in the potentials into the Schrödinger equation (cf. section 4.3) to find a bound state, we have to fit a continuous function to the lattice results. We are proceeding analogous to [5], where the following ansatz is used:

$$V(r) = -\frac{\alpha}{r} \exp\left[-\left(\frac{r}{d}\right)^p\right] \tag{4.2}$$

In this work we are using a two parameter fit (α,d) to determine the respective potentials. Due to the considerations made in [5], the value of p is set for all concerning calculations each to 1.0, 1.5 and 2.0.

During the creation of this work the potentials to all quantum numbers listed in Appendix A were computed both for s and for c quarks. The qualitative behaviour of these potentials, i.e. repulsive (rep) or attractive (att), does not depend on the quark mass and can be taken from the tables shown in Appendix A as well.

In order to compare the results with [5], we are only focussing in detail on the two most attractive channels, the scalar isosinglet and the vector isotriplet. The corresponding creation operators for the scalar isosinglet entails $\Gamma^{(\mathrm{ppb})} = \gamma_5 + \gamma_0\gamma_5$ with light quark flavour combination $ud - du$.

The vector isotriplet can be described by the creation operator entailing $\Gamma^{(\mathrm{ppb})} = \gamma_0\gamma_3 + \gamma_3$ and light quark flavour combination $ud + du$. The degenerate isospin partners with light quark flavour combination ud/du yield the same quantum numbers and thus we included the corresponding results into those we used for the fitting procedure.

4.2.1 Charm quarks

A meson consisting of a static antiquark and a charm quark corresponds to a so called B_c meson, which is built up from an $\bar{b}$ and a c quark. Hence, the following potentials are called B_cB_c potentials.

Regarding (2.9) and (2.10), it is important to fit the mass plateaus at large times T. However, this is not always possible, since the statistical errors increase at high values of T, which restricts the fitting range significantly.

Nevertheless, the signal for the meson masses was rather precise, so we were able to determine the meson masses at a comparatively high precision. But this was not the case for the B_cB_c potentials, especially not for the results without HYP2 smearing.

We performed the fits for the mass plateaus of the potentials at the same time span for the HYP2 smeared and the unsmeared results, which was the largest possible range for the unsmeared results. Performing the plateau fits for the meson masses at that time span yielded values for the χ^2-error of over 150 and thus, we performed the fits for the meson masses at larger ranges. Subtracting two times the corresponding B_c meson mass (each with and without HYP2 smearing, respectively) should set the plateau, which the potentials approach, to 0. Regarding Figure 4.1, this is obviously not the case.

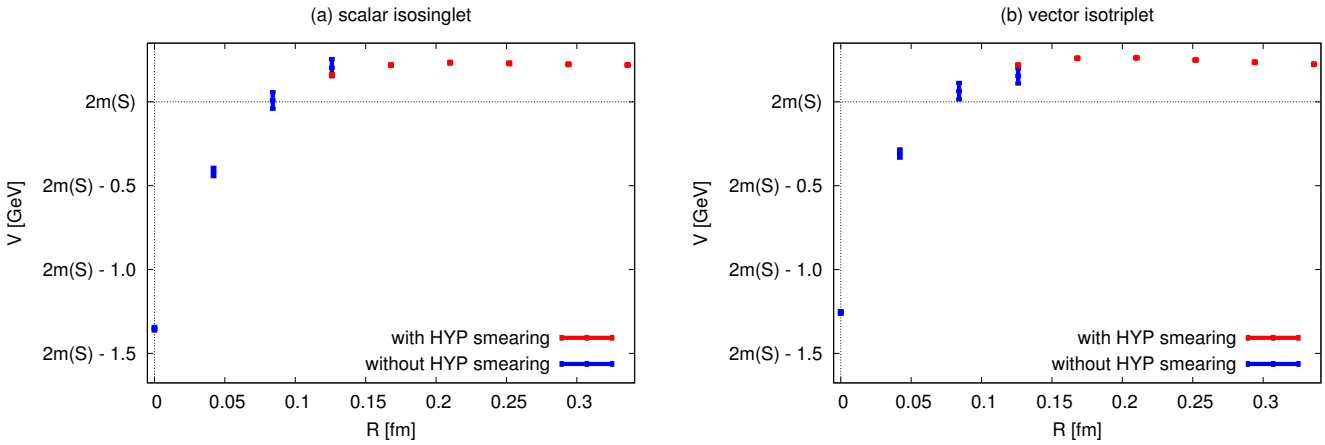

Figure 4.1: B_cB_c potentials for the scalar isosinglet (a) and the vector isotriplet (b) both with and without HYP smearing (not adjusted)

The reason for the too high potential values is the fact that the effective masses within the potentials do not reach the mass plateaus for this short time range and thus higher excitations are sizeable included. In addition, as mentioned above, we used a larger time span for the plateau fits for the meson masses, which also increases the discrepancy. However, we were able to fit the effective masses within the potentials at larger time ranges for the HYP2 smeared results, which lowers the values of the corresponding potentials to the expected value of two times the meson mass within the range of the statistical errors.

Nevertheless, there is also an alternative strategy. Assuming the same behaviour for the potential using the unsmeared links, we adjusted the appropriate normalisation constant so that the potential values match at $R = 3a$. Furthermore, we shifted the plateaus, which the potentials approach, to the corresponding value of $2m(S)$. This is shown in Figure 4.2.

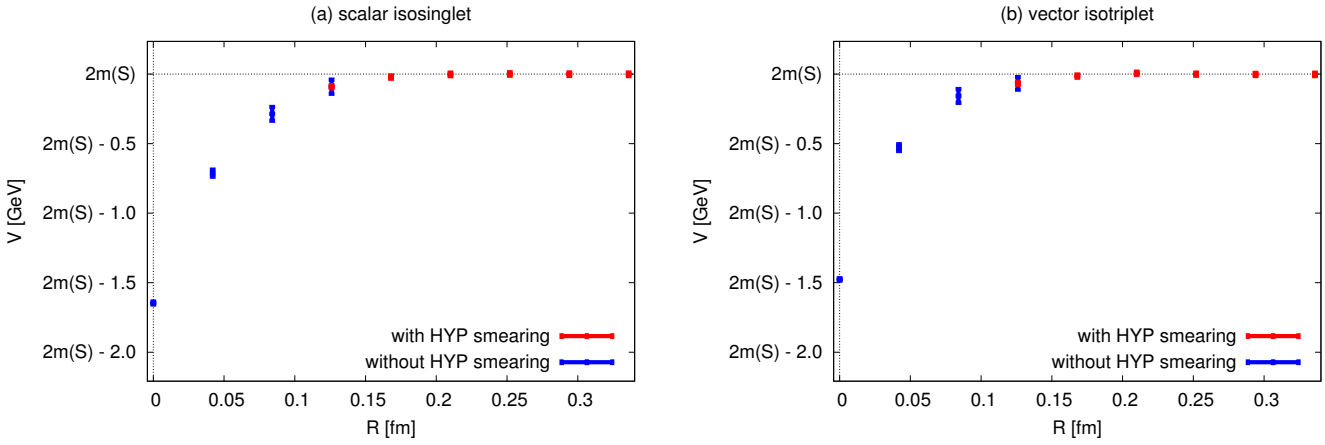

Figure 4.2: B_cB_c potentials for the scalar isosinglet (a) and the vector isotriplet (b) both with and without HYP smearing (adjusted)

Applying the ansatz (4.2) with $p = 2.0$ to the lattice results shown in Figure 4.2 yields the continuous potential $V(r)$, which is presented in Figure 4.3. The potential fits for the p-values 1.0 and 1.5 can be taken from Appendix B.

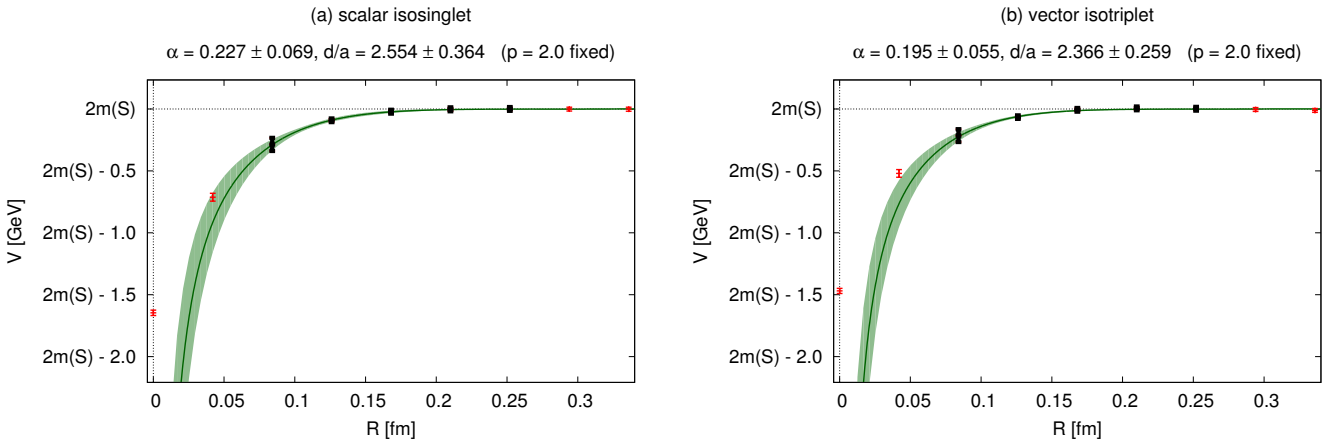

Figure 4.3: Fitted B_cB_c potentials for the scalar isosinglet (a) and the vector isotriplet (b) with $p = 2.0$ fixed (red points not included into the fit)

4.2.2 Strange quarks

Analogous to the previous subsection, the potential between two mesons, each consisting of a static antiquark and a strange quark, corresponds to the potential between two B_s mesons.

Using strange quarks involves higher statistical errors compared to the previous computations with charm quarks, since the strange quark mass is considerably smaller than the charm quarks mass. The statistical errors of the potential values at $R = 3a$ for the results without HYP2 smearing were so large that they were unusable. Thus, we already matched the potentials at $R = 2a$ and used the potential values of the results with HYP2 smeared links for $R \geq 3a$.

The adjusted potentials for the scalar isosinglet and the vector isotriplet are presented in Figure 4.4 and the corresponding potential fits according to (4.2) are shown in Figure 4.5.

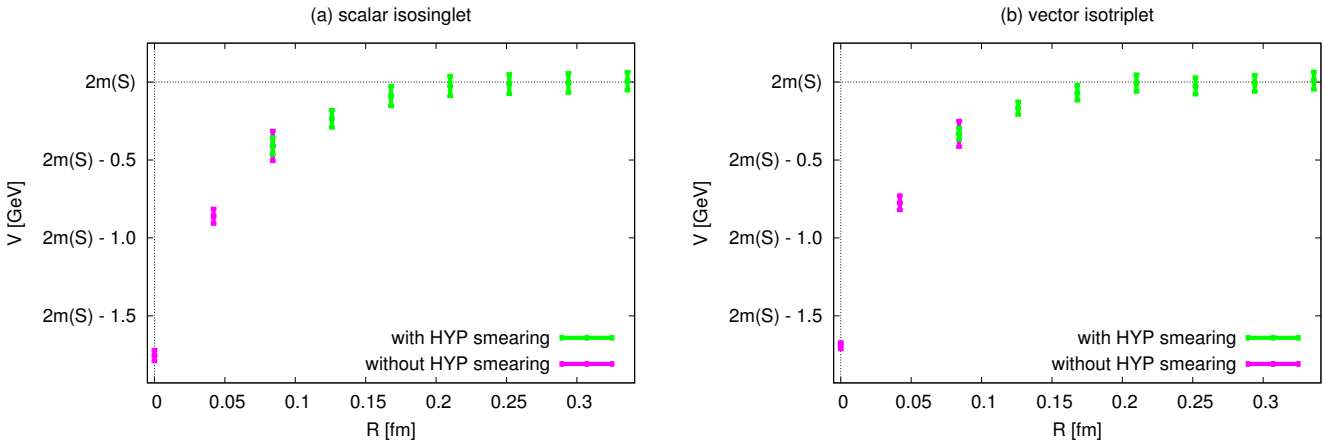

Figure 4.4: B_sB_s potentials for the scalar isosinglet (a) and the vector isotriplet (b) both with and without HYP smearing (adjusted)

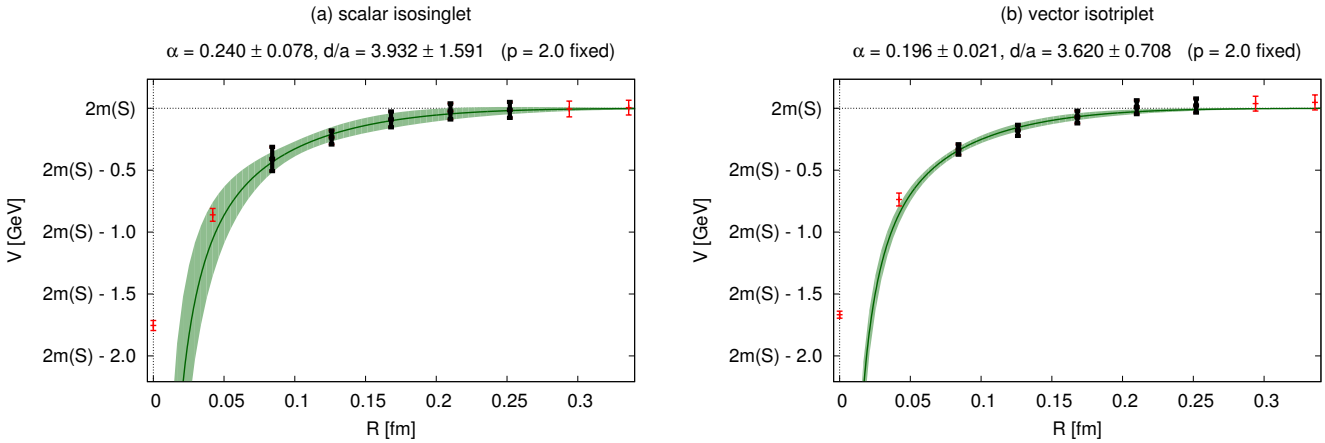

Figure 4.5: Fitted B_sB_s potentials for the scalar isosinglet (a) and the vector isotriplet (b) with $p = 2.0$ fixed (red points not included into the fit)

As mentioned in the beginning of this section, we only included the degenerate isospin partners of the vector isotriplet into the fitted potentials (Figure 4.5) but not into the potentials shown in Figure 4.4. This leads to small fluctuations of the potential values, but within the respective error margins.

4.2.3 Comparison with light quarks

To compare the results for the considered s and c quarks, the different potentials are plotted with the results taken from [5] for light quarks in Figure 4.6.

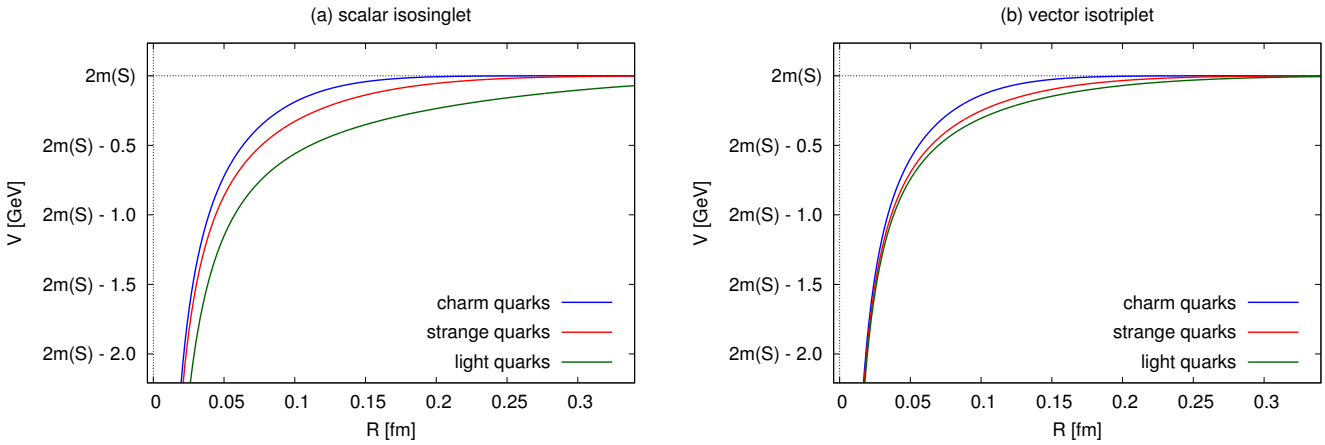

Figure 4.6: Comparison between the $\bar{Q}\bar{Q}$ potentials for the different considered quarks (without error bars)

The results for the light quarks were transformed into physical units by setting the lattice spacing to $a = 0.079\,\text{fm}$, like proposed in [5].

As expected, the potential gets more narrow, if the quark mass increases. It is noticeable that in (a) the potential for strange quarks is closer to that for charm quarks and in (b) it is closer to that for light quarks. Nevertheless, this is within the error margin, which is not shown in Figure 4.6 for reasons of clarity, but can be seen in Figure 4.3 and Figure 4.5.

4.3 Numerical solution of the Schrödinger equation

In this section we will solve the Schrödinger equation numerically in order to find out whether there is an indication for a bound B_cB_c/B_sB_s state, i.e. a tetraquark, or not. We are proceeding analogous to [5].

Obviously, if the two antiquarks $\bar{Q}$, which are treated in the static limit, were infinitely heavy, they would form an arbitrary large binding energy in all attractive channels. Nevertheless, they have a finite mass so the binding is questionable. To see if there is a bound tetraquark state we solve the s-wave radial part of the Schrödinger equation for the fitted potentials $V(r)$, i.e.

$$\left[-\frac{\hbar}{2\mu}\frac{d^2}{dr^2} + 2m_M + V(r)\right] R(r) = ER(r)\,, \tag{4.3}$$

with the wave function $\psi(r) = \frac{R(r)}{r}$ and the meson mass $m_M \in \{m_{B_s}, m_{B_c}\}$. The reduced quark mass μ is both set to $\frac{m_M}{2}$ and $\frac{m_b}{2}$, where m_b is the mass of a bottom quark. This is because each

heavy antiquark carries for small separations only the bottom quark mass, but for large separations the mass of the respective meson. The used mass values are listed in Table 4.3.

m_b	m_{B_s}	m_{B_c}
4977 MeV	5367 MeV	6277 MeV

Table 4.3: Values for the different quark and meson masses used in this work (cf. [2, 18])

Solving the Schrödinger equation (4.3) yields neither a bound state for charm quarks nor for strange quarks. In order to be able to better assess this result, we determined how far we would have to increase the inserted masses listed in Table 4.3 to reach binding.

For the potentials with c quarks the inserted mass should be $\gtrsim 10\, m_{B_c}$ for the scalar isosinglet and even larger for the vector isotriplet. Concerning s quarks, the inserted mass should be $\gtrsim 1.7\, m_{B_s}$ for both channels.

This indicates that it is extremely improbable to find a bound B_cB_c state, i.e. a $bb\bar{c}\bar{c}$ tetraquark. For the case with s quarks, it also seems evidenced that even bearing in mind the systematic errors arising during the potential normalisation (cf. subsection 4.2.2) there is no indication for a bound B_sB_s state, i.e. a $bb\bar{s}\bar{s}$ tetraquark.

These results clearly indicate that increasing the quark mass decreases the chance of finding a bound tetraquark state. Hence, the effect that the potential becomes more narrow outweighs the fact that heavier constituents do easier form a bound state.

4.4 $\bar{Q}Q$ potentials

This section shows the first results of the computations done for the potential between a meson consisting of a static antiquark $\bar{Q}$ and a quark of finite mass and another meson which is made of a static quark Q and an antiquark of finite mass.

4.4.1 Charm quarks

Since this is meant to be a first test and we want to focus on the qualitative behaviour of the potentials, i.e. see if the potentials are attractive or repulsive, we used the smaller lattice A40.24 (c.f. Table 4.1) and charm quarks to reduce the computation time. This means that the following potentials correspond to the potentials between a B_c and a $\bar{B}_c$ meson. In addition, the results are presented in units of the lattice spacing a.

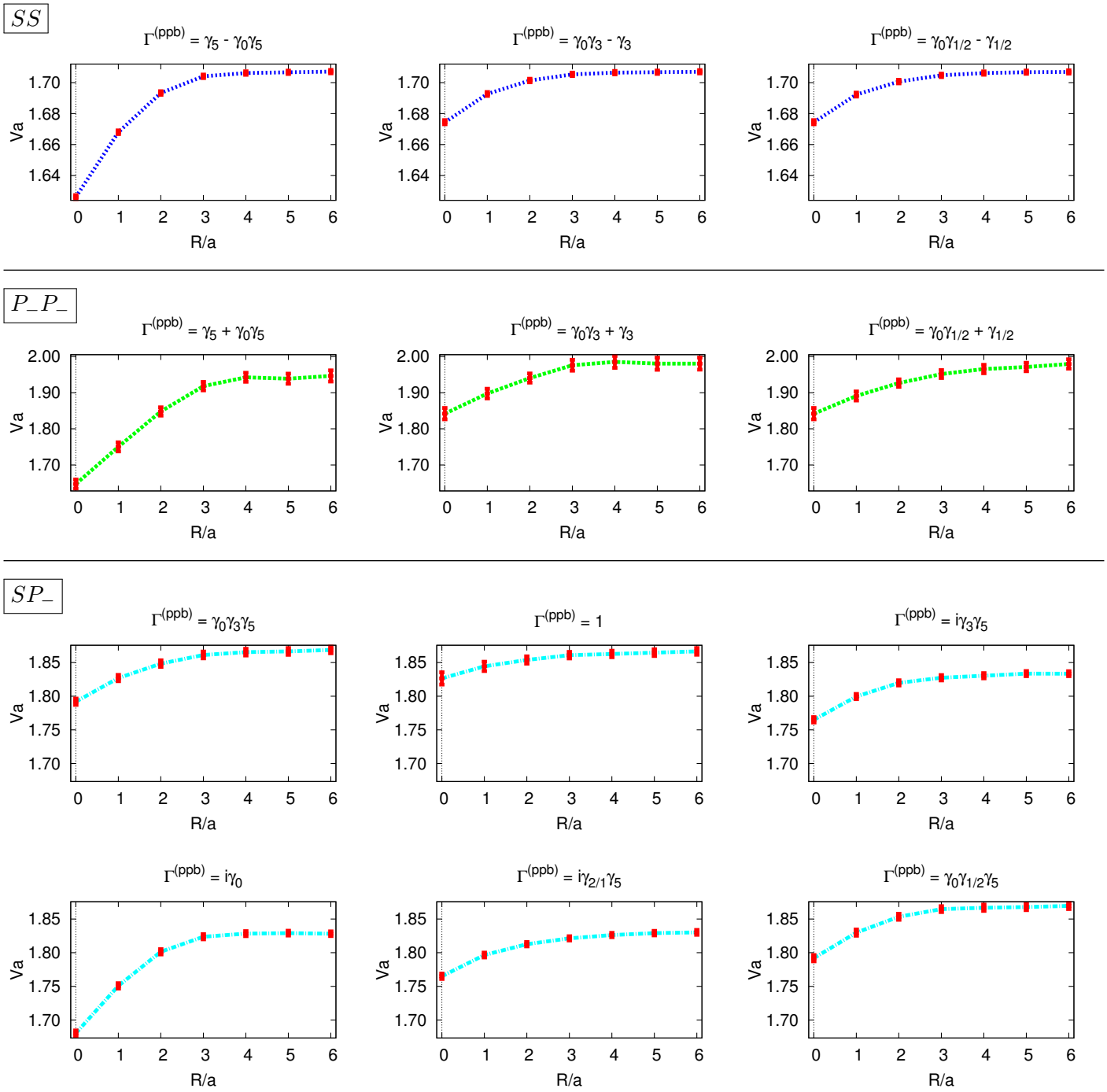

Figure 4.7: $B_c\bar{B}_c$ potentials with light flavour combination $u\bar{d}$ (i.e. $I = 1$) sorted by their meson content for the different Γ matrices with corresponding quantum numbers listed in Table 2.6 (lattice units)

In accordance to the previous considerations in section 2.5 the potentials pictured in Figure 4.7 saturate at three different levels. The potentials shown in the first row saturate at the smallest value of $Va \approx 1.7$, which is in the range of two times the mass of the lightest static-charm meson state S (cf. Figure 4.8, which shows two effective mass plots with appropriate plateau fits for the static-light meson states S and P_-).

The potentials shown in the second row of Figure 4.7 saturate at the highest level of $Va \approx 2.0$. This value is in the range of the static-charm meson mass of the excited P_- state and thus again compatible with the preliminary consideration concerning the meson content in section 2.5.

The meson content of the six potentials at the bottom of Figure 4.7 is a combination of S and P_- static-charm mesons. Hence, they should saturate at approximately $m(S) + m(P_-)$, which is also fulfilled.

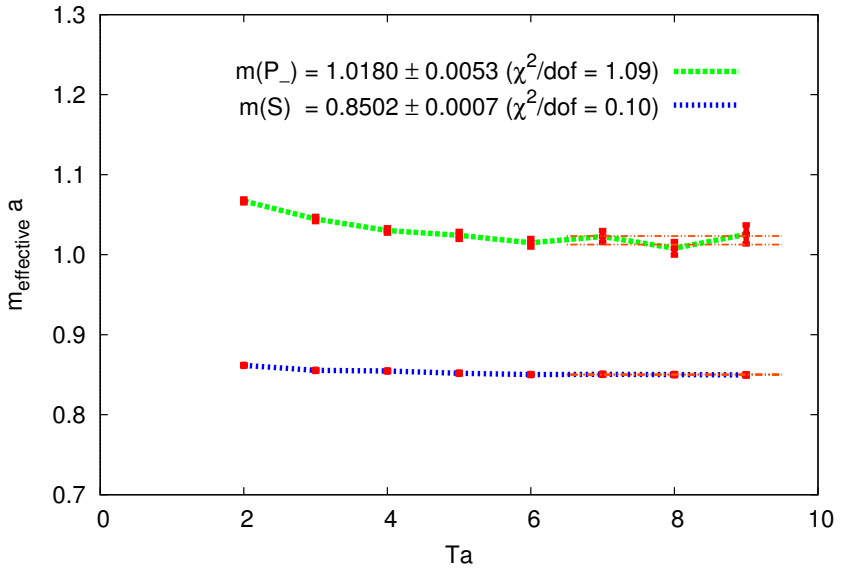

Figure 4.8: Effective masses of static-charm mesons and the corresponding mass plateau fits for ensemble A40.24 (lattice units)

4.4.2 Comparison with B_cB_c

The most crucial outcome of the studies concerning $B_c\bar{B}_c$ potentials is the fact that all potentials are attractive. Regarding B_cB_c systems, both attractive and repulsive potentials occurred (cf. subsection 4.2.1 and Figure 4.9, respectively).

Although, we only checked this statement for half of the potentials, i.e. for those with $I = 1$, this seems to hold for $I = 0$ as well. The reason for this is the fact that changing only one of the quantum numbers like flavour, spin or parity, flips the potential from attractive to repulsive and vice versa in the case of BB. Since we are considering all quantum numbers in the $I = 1$ channel, this rule is for $B\bar{B}$ not valid and therefore there is no indication for repulsive potentials in the $I = 0$ channel.

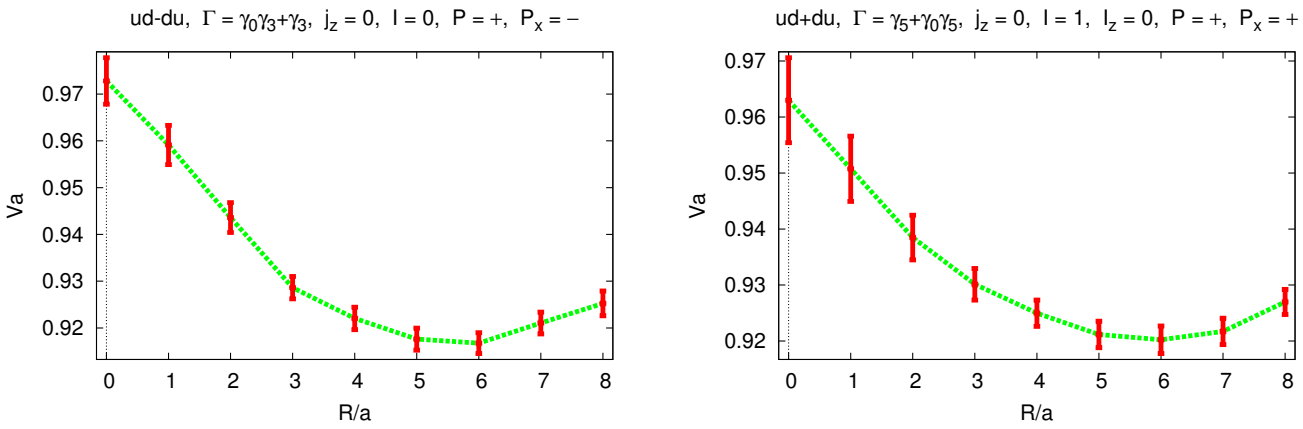

Figure 4.9: Two examples for repulsive B_cB_c potentials (lattice units)

A possible explanation from a more phenomenological point of view is given in [19], where the argumentation is mainly based on the Pauli principle. Starting from colour singlets B_c, the colour wave function of the two indistinguishable antiquarks $\bar{b}$ within the B_cB_c system is either in a triplet, which is attractive, or an anti-sextet, which is repulsive. For $B_c\bar{B}_c$, again starting form colour singlets $B_c/\bar{B}_c$, the colour wave function of the $b\bar{b}$ pair can either be in a singlet, which is attractive, or in an octet, which is repulsive.

The difference is, that due to the Pauli principle and conservation of the initial quantum numbers, there are specific channels for B_cB_c where only the repulsive anti-sextet can be achieved. This leads to repulsive potentials as shown in Figure 4.9. However, for $B_c\bar{B}_c$ the ground state is always a singlet, which yields attractive potentials (cf. Figure 4.7).

Chapter 5

Conclusion

5.1 Summary

In this work we expanded the investigations of [3–5], where the potentials between two static-light mesons were studied, i.e. $\bar{Q}\bar{Q}$ potentials, in two ways:

- We computed the $\bar{Q}\bar{Q}$ potentials both for charm and for strange quarks in order to analyse the behaviour of the potentials depending on the quark mass and to check if there are also indications for a bound tetraquark state.
- We took initial steps towards extending the $\bar{Q}\bar{Q}$ investigations to the experimentally more interesting case of $\bar{Q}Q$.

The results for the $\bar{Q}\bar{Q}$ potentials clearly indicate that there are no bound $\bar{b}\bar{b}ss$ and $\bar{b}\bar{b}cc$ tetraquark states. Another outcome concerning these $\bar{Q}\bar{Q}$ investigations is that increasing the quark mass decreases the chance of finding a bound tetraquark state.

The investigations of the $\bar{Q}Q$ systems yielded remarkable results regarding the qualitative behaviour of the different potentials. In contrast to the $\bar{Q}\bar{Q}$ potentials, the $\bar{Q}Q$ potentials are all attractive.

5.2 Oulook

With the results of this work and those of [3–5] the investigations of $\bar{Q}\bar{Q}$ potentials seem to be completed. However, e.g. the continuum limit and lighter quark masses could be considered. In addition, an improvement could of course be made by reducing the statistical errors. This can be done by increasing the number of the inversions per gauge field configuration, the size of the lattice or by just using more gauge field configurations.

The investigations of the $\bar{Q}Q$ systems should be extended as a next step by means of the missing box diagrams to compute the remaining half of the problem, i.e. the potentials for $I = 0$. Furthermore, strange and light quarks could be considered.

An additional step would be the computation of the existing potentials with reduced statistical errors in the same way as mentioned above, so that a sensible potential fit can be performed. Afterwards one could check if there are indications for a bound tetraquark state, as was done for the $\bar{Q}\bar{Q}$ systems.

Appendix A

BB systems

A.1 Quantum numbers

In the following, the different quantum numbers for BB systems are listed in two tables. Table A.1 shows those for the flavour combination uu/dd and Table A.2 those for the flavour combination $ud \pm du$. A respective detailed discussion is made for $B\bar{B}$ systems in section 2.6.

$\Gamma^{\binom{uu}{dd}}$ tb	$\mathscr{P}^{(\mathrm{tm})}$	sec.	$\Gamma^{\binom{uu}{dd}}$ ppb	$\mathscr{P}$, $\mathscr{P}_x$	type	mult.
$j_z = 0,\ I = 1,\ I_z = \pm 1$						
$\gamma_3 \pm i\gamma_0\gamma_3\gamma_5$	$+$	i	$+\gamma_3 + \gamma_0\gamma_3$	$-,\ -$	att SS	E
γ_5	$+$	i	$\mp i$	$-,\ -$	rep SP_-	E
$\gamma_3 \mp i\gamma_0\gamma_3\gamma_5$	$+$	i	$+\gamma_3 - \gamma_0\gamma_3$	$-,\ -$	att P_-P_-	E
$\gamma_0\gamma_5 \pm i$	$+$	i	$+\gamma_0\gamma_5 + \gamma_5$	$+,\ +$	rep SS	F
$\gamma_0\gamma_3$	$+$	i	$\mp i\gamma_0\gamma_3\gamma_5$	$+,\ +$	att SP_-	F
$\gamma_0\gamma_5 \mp i$	$+$	i	$+\gamma_0\gamma_5 - \gamma_5$	$+,\ +$	rep P_-P_-	F
γ_0	$-$	j	$+\gamma_0$	$+,\ -$	att SP_-	G
$\gamma_3\gamma_5$	$-$	j	$+\gamma_3\gamma_5$	$-,\ +$	rep SP_-	H
$j_z = 1,\ I = 1,\ I_z = \pm 1$						
$\gamma_{1/2} \pm i\gamma_0\gamma_{1/2}\gamma_5$	$-/+$	k/l	$+\gamma_{1/2} + \gamma_0\gamma_{1/2}$	$-,\ +/-$	att SS	K
$\gamma_{2/1}\gamma_5$	$-/+$	k/l	$+\gamma_{2/1}\gamma_5$	$-,\ +/-$	rep SP_-	K
$\gamma_{1/2} \mp i\gamma_0\gamma_{1/2}\gamma_5$	$-/+$	k/l	$+\gamma_{1/2} - \gamma_0\gamma_{1/2}$	$-,\ +/-$	att P_-P_-	K
$\gamma_0\gamma_{1/2}$	$-/+$	k/l	$\mp i\gamma_0\gamma_{1/2}\gamma_5$	$+,\ -/+$	att SP_-	L

Table A.1: Twisted and physical quantum numbers for uu/dd (taken from [20])

$\Gamma^{(ud\pm du)}$ tb	$\mathscr{P}^{(\mathrm{tm})}$, $\mathscr{P}_x^{(\mathrm{tm})}$	sec.	$\Gamma^{(ud\pm du)}$ ppb	$\mathscr{P}$, $\mathscr{P}_x$	type	mult.
$j_z = 0,\ I = 0$						
$\gamma_5^{(-)} - i\gamma_0^{(+)}$	$+,\ -$	a	$(+\gamma_5 + \gamma_0\gamma_5)^{(-)}$	$-,\ +$	att SS	A
$\gamma_0\gamma_3\gamma_5^{(-)}$	$+,\ -$	a	$+\gamma_0\gamma_3\gamma_5^{(-)}$	$-,\ +$	rep SP_-	A
$\gamma_5^{(-)} + i\gamma_0^{(+)}$	$+,\ -$	a	$(+\gamma_5 - \gamma_0\gamma_5)^{(-)}$	$-,\ +$	att P_-P_-	A
$\gamma_0\gamma_3^{(-)} - i\gamma_3\gamma_5^{(+)}$	$-,\ +$	b	$(+\gamma_0\gamma_3 + \gamma_3)^{(-)}$	$+,\ -$	rep SS	B
$1^{(-)}$	$-,\ +$	b	$+1^{(-)}$	$+,\ -$	att SP_-	B
$\gamma_0\gamma_3^{(-)} + i\gamma_3\gamma_5^{(+)}$	$-,\ +$	b	$(+\gamma_0\gamma_3 - \gamma_3)^{(-)}$	$+,\ -$	rep P_-P_-	B
$\gamma_3^{(+)}$	$-,\ -$	c	$+i\gamma_3\gamma_5^{(-)}$	$+,\ +$	att SP_-	C
$\gamma_0\gamma_5^{(+)}$	$+,\ +$	d	$+i\gamma_0^{(-)}$	$-,\ -$	rep SP_-	D
$j_z = 0,\ I = 1,\ I_z = 0$						
$\gamma_0\gamma_3^{(+)} - i\gamma_3\gamma_5^{(-)}$	$-,\ -$	c	$(+\gamma_0\gamma_3 + \gamma_3)^{(+)}$	$-,\ -$	att SS	E
$1^{(+)}$	$-,\ -$	c	$+1^{(+)}$	$-,\ -$	rep SP_-	E
$\gamma_0\gamma_3^{(+)} + i\gamma_3\gamma_5^{(-)}$	$-,\ -$	c	$(+\gamma_0\gamma_3 - \gamma_3)^{(+)}$	$-,\ -$	att P_-P_-	E
$\gamma_5^{(+)} - i\gamma_0^{(-)}$	$+,\ +$	d	$(+\gamma_5 + \gamma_0\gamma_5)^{(+)}$	$+,\ +$	rep SS	F
$\gamma_0\gamma_3\gamma_5^{(+)}$	$+,\ +$	d	$+\gamma_0\gamma_3\gamma_5^{(+)}$	$+,\ +$	att SP_-	F
$\gamma_5^{(+)} + i\gamma_0^{(-)}$	$+,\ +$	d	$(+\gamma_5 - \gamma_0\gamma_5)^{(+)}$	$+,\ +$	rep P_-P_-	F
$\gamma_0\gamma_5^{(-)}$	$+,\ -$	a	$+i\gamma_0^{(+)}$	$+,\ -$	att SP_-	G
$\gamma_3^{(-)}$	$-,\ +$	b	$+i\gamma_3\gamma_5^{(+)}$	$-,\ +$	rep SP_-	H
$j_z = 1,\ I = 0$						
$\gamma_0\gamma_{1/2}^{(-)} - i\gamma_{1/2}\gamma_5^{(+)}$	$-,\ -/+$	e/f	$(+\gamma_0\gamma_{1/2} + \gamma_{1/2})^{(-)}$	$+,\ +/-$	rep SS	I
$\gamma_{2/1}^{(+)}$	$-,\ -/+$	e/f	$+i\gamma_{2/1}\gamma_5^{(-)}$	$+,\ +/-$	att SP_-	I
$\gamma_0\gamma_{1/2}^{(-)} + i\gamma_{1/2}\gamma_5^{(+)}$	$-,\ -/+$	e/f	$(+\gamma_0\gamma_{1/2} - \gamma_{1/2})^{(-)}$	$+,\ +/-$	rep P_-P_-	I
$\gamma_0\gamma_{1/2}\gamma_5^{(-)}$	$+,\ +/-$	g/h	$\gamma_0\gamma_{1/2}\gamma_5^{(-)}$	$-,\ -/+$	rep SP_-	J
$j_z = 1,\ I = 1,\ I_z = 0$						
$\gamma_0\gamma_{1/2}^{(+)} - i\gamma_{1/2}\gamma_5^{(-)}$	$-,\ +/-$	f/e	$(+\gamma_0\gamma_{1/2} + \gamma_{1/2})^{(+)}$	$-,\ +/-$	att SS	K
$\gamma_{2/1}^{(-)}$	$-,\ +/-$	f/e	$+i\gamma_{2/1}\gamma_5^{(+)}$	$-,\ +/-$	rep SP_-	K
$\gamma_0\gamma_{1/2}^{(+)} + i\gamma_{1/2}\gamma_5^{(-)}$	$-,\ +/-$	f/e	$(+\gamma_0\gamma_{1/2} - \gamma_{1/2})^{(+)}$	$-,\ +/-$	att P_-P_-	K
$\gamma_0\gamma_{1/2}\gamma_5^{(+)}$	$+,\ -/+$	h/g	$\gamma_0\gamma_{1/2}\gamma_5^{(+)}$	$+,\ -/+$	att SP_-	L

Table A.2: Twisted and physical quantum numbers for $ud \pm du$ (taken from [20])

A.2 Meson content

Table A.3 shows the meson content of a BB system depending on the Γ choice. More information about the meson content in the case of $B\bar{B}$ systems can be taken from section 2.5.

Γ (pseudo) physical	meson content
γ_5	$-S_\uparrow S_\downarrow + S_\downarrow S_\uparrow - P_\uparrow P_\downarrow + P_\downarrow P_\uparrow$
$\gamma_0\gamma_5$	$-S_\uparrow S_\downarrow + S_\downarrow S_\uparrow + P_\uparrow P_\downarrow - P_\downarrow P_\uparrow$
1	$-S_\uparrow P_\downarrow + S_\downarrow P_\uparrow - P_\uparrow S_\downarrow + P_\downarrow S_\uparrow$
γ_0	$-S_\uparrow P_\downarrow + S_\downarrow P_\uparrow + P_\uparrow S_\downarrow - P_\downarrow S_\uparrow$
γ_3	$-iS_\uparrow S_\downarrow - iS_\downarrow S_\uparrow + iP_\uparrow P_\downarrow + iP_\downarrow P_\uparrow$
$\gamma_0\gamma_3$	$-iS_\uparrow S_\downarrow - iS_\downarrow S_\uparrow - iP_\uparrow P_\downarrow - iP_\downarrow P_\uparrow$
$\gamma_3\gamma_5$	$-iS_\uparrow P_\downarrow - iS_\downarrow P_\uparrow + iP_\uparrow S_\downarrow + iP_\downarrow S_\uparrow$
$\gamma_0\gamma_3\gamma_5$	$-iS_\uparrow P_\downarrow - iS_\downarrow P_\uparrow - iP_\uparrow S_\downarrow - iP_\downarrow S_\uparrow$
γ_1	$+iS_\uparrow S_\uparrow - iS_\downarrow S_\downarrow - iP_\uparrow P_\uparrow + iP_\downarrow P_\downarrow$
$\gamma_0\gamma_1$	$+iS_\uparrow S_\uparrow - iS_\downarrow S_\downarrow + iP_\uparrow P_\uparrow - iP_\downarrow P_\downarrow$
$\gamma_1\gamma_5$	$+iS_\uparrow P_\uparrow - iS_\downarrow P_\downarrow - iP_\uparrow S_\uparrow + iP_\downarrow S_\downarrow$
$\gamma_0\gamma_1\gamma_5$	$+iS_\uparrow P_\uparrow - iS_\downarrow P_\downarrow + iP_\uparrow S_\uparrow - iP_\downarrow S_\downarrow$
γ_2	$-S_\uparrow S_\uparrow - S_\downarrow S_\downarrow + P_\uparrow P_\uparrow + P_\downarrow P_\downarrow$
$\gamma_0\gamma_2$	$-S_\uparrow S_\uparrow - S_\downarrow S_\downarrow - P_\uparrow P_\uparrow - P_\downarrow P_\downarrow$
$\gamma_2\gamma_5$	$-S_\uparrow P_\uparrow - S_\downarrow P_\downarrow + P_\uparrow S_\uparrow + P_\downarrow S_\downarrow$
$\gamma_0\gamma_2\gamma_5$	$-S_\uparrow P_\uparrow - S_\downarrow P_\downarrow - P_\uparrow S_\uparrow - P_\downarrow S_\downarrow$

Table A.3: Relation between Γ in the (pseudo) physical basis and the static-light meson content (taken from [20])

Appendix B

$\bar{Q}\bar{Q}$ potentials

B.1 B_cB_c

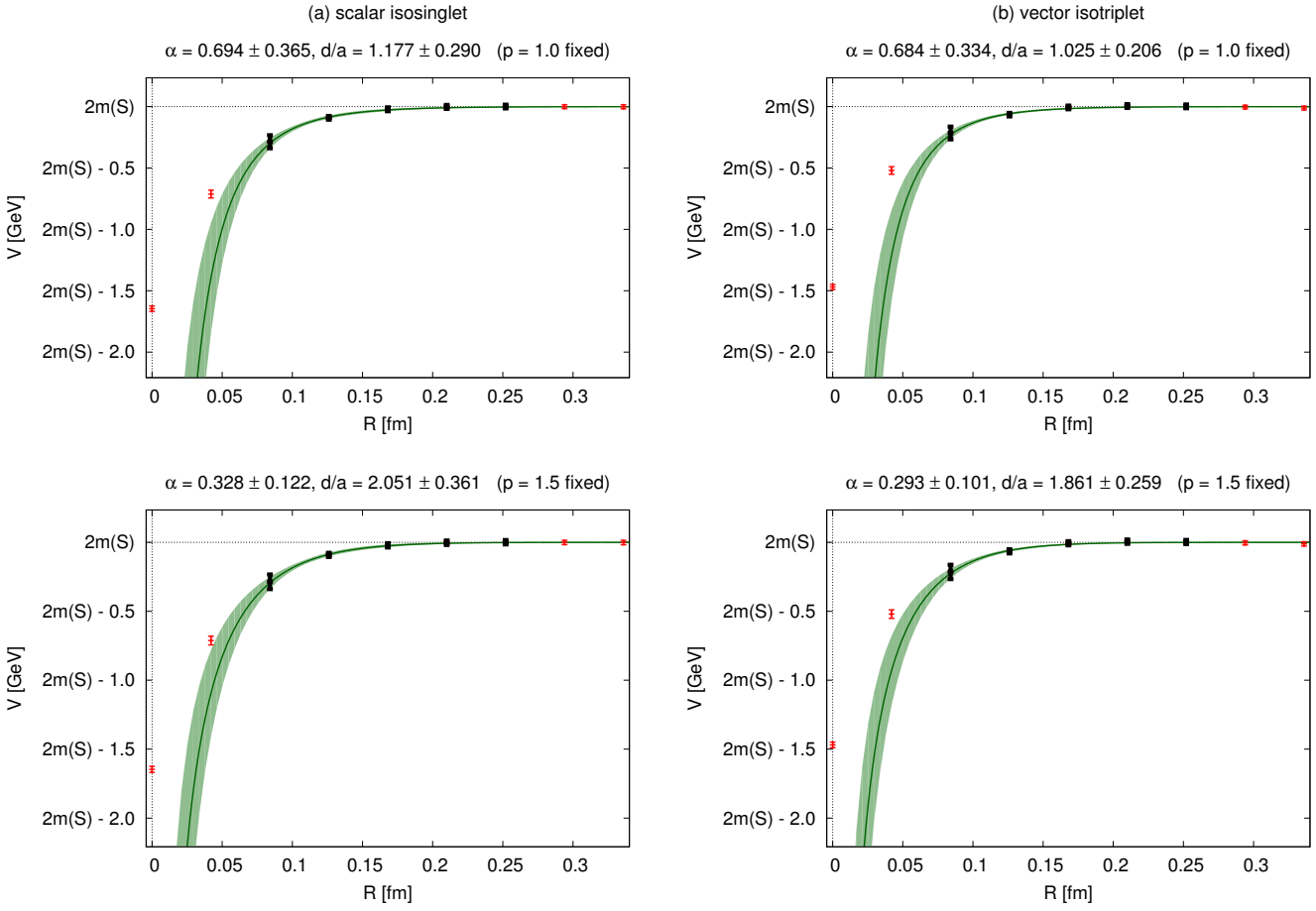

Figure B.1: Fitted B_cB_c potentials for the scalar isosinglet (a) and the vector isotriplet (b) with fixed p-values 1.0 and 1.5 (red points not included into the fit), cf. subsection 4.2.1

B.2 B_sB_s

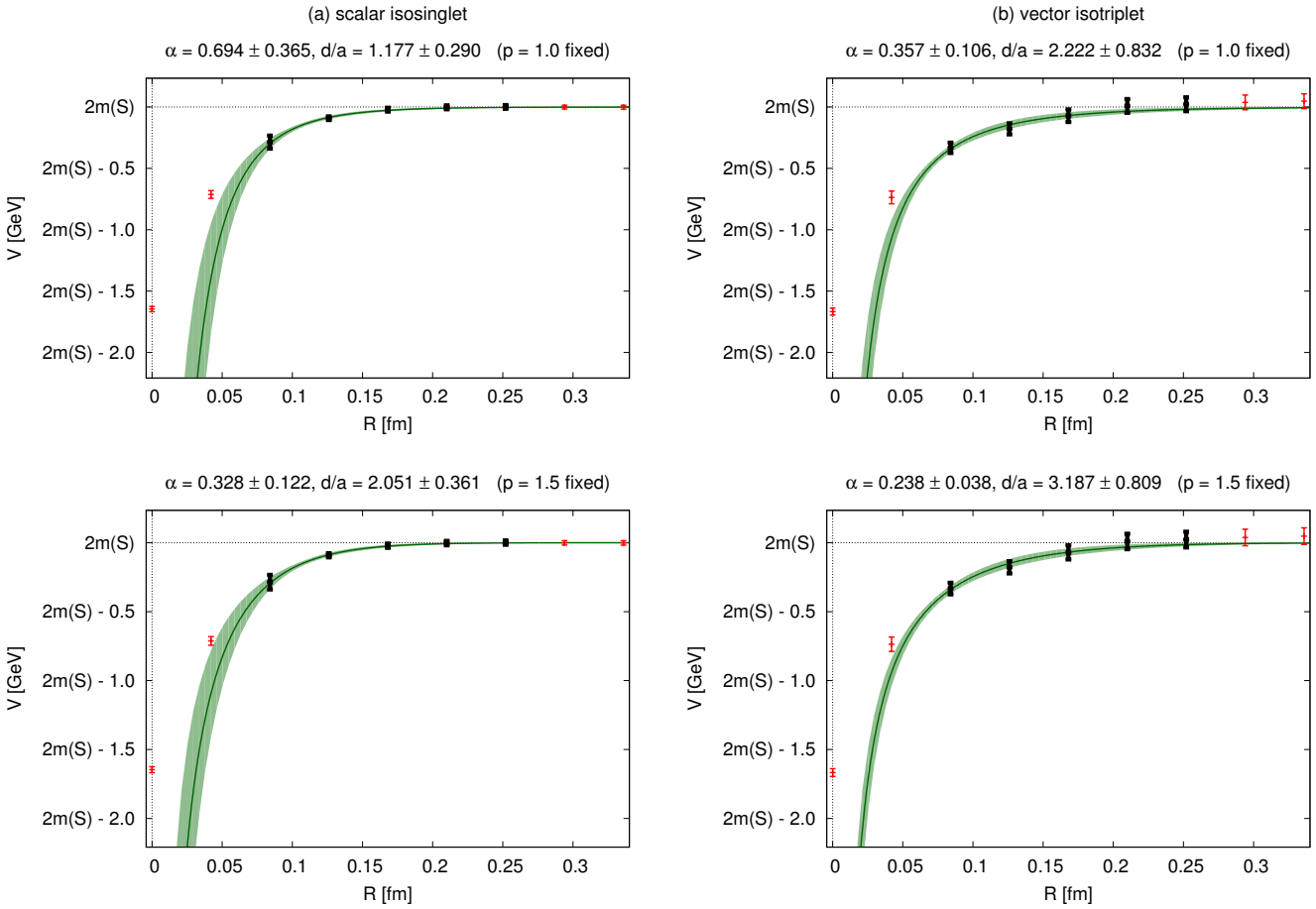

Figure B.2: Fitted B_sB_s potentials for the scalar isosinglet (a) and the vector isotriplet (b) with fixed p-values 1.0 and 1.5 (red points not included into the fit), cf. subsection 4.2.2

References

[1] R. L. Jaffe, Phys. Rev. D 15, 267 (1977).

[2] J. Beringer, Phys. Rev. D 86, 010001 (2012).

[3] M. Wagner [ETM Collaboration], PoS LATTICE2010, 162 (2010) [arXiv:1008.1538 [hep-lat]].

[4] M. Wagner [ETM Collaboration], Acta Phys. Polon. Supp. 4, 747 (2011) [arXiv:1103.5147 [hep-lat]].

[5] P. Bicudo and M. Wagner, Phys. Rev. D 87, 114511 (2013) [arXiv:1209.6274 [hep-ph]].

[6] A. Shindler, Phys. Rept. 461, 37 (2008) [arXiv:0707.4093 [hep-lat]].

[7] C. Alexandrou, J. O. Daldrop, M. D. Brida, M. Gravina, L. Scorzato, C. Urbach and M. Wagner, JHEP 1304, 137 (2013) [arXiv:1212.1418 [hep-lat]].

[8] R. Baron et al. [ETM Collaboration], Comput. Phys. Commun. 182, 299 (2011) [arXiv:1005.2042 [hep-lat]].

[9] R. Frezzotti and G. C. Rossi, JHEP 0408, 007 (2004) [hep-lat/0306014].

[10] K. Nakamura et al. [Particle Data Group], J. Phys. G 37, 075021 (2010).

[11] K. Jansen, C. Michael, A. Shindler and M. Wagner [ETM Collaboration], JHEP 0812, 058 (2008) [arXiv:0810.1843 [hep-lat]].

[12] C. Michael, A. Shindler and M. Wagner [ETM Collaboration], JHEP 1008, 009 (2010) [arXiv:1004.4235 [hep-lat]].

[13] P. Boucaud et al. [ETM Collaboration], Comput. Phys. Commun. 179, 695 (2008) [arXiv:0803.0224 [hep-lat]].

[14] S. J. Dong and K. F. Liu, Phys.Lett. B 328, 130-136 (1994) [arXiv:hep-lat/9308015].

[15] R. Baron et al., JHEP 1006, 111 (2010) [arXiv:1004.5284 [hep-lat]].

[16] K. Cichy et al., Nucl.Phys. B 865, 268-290 (2012) [arXiv:1207.0628 [hep-lat]].

[17] K. Jansen, C. Michael, A. Shindler and M. Wagner [ETM Collaboration], JHEP 0812, 058 (2008) [arXiv:0810.1843 [hep-lat]].

[18] S. Godfrey and N. Isgur, Phys. Rev. D 32, 189 (1985).

[19] P. Bicudo, *private notes/unpublished.*

[20] M. Wagner, *private notes/unpublished.*

Danksagung

Besonderen Dank möchte ich Prof. Marc Wagner für die hervorragende Betreuung aussprechen. Aus den häufigen Diskussionen habe ich sehr viel mitnehmen können und auch die vielen Tipps und Raschläge haben maßgeblich zur Gestaltung der vorliegenden Arbeit beigetragen.

Auch Prof. Owe Philipsen möchte ich an dieser Stelle für die Übernahme des Zweitprüferamtes und das Ermöglichen einer nahtlosen Fortsetzung meiner akademische Laufbahn danken.

Desweiteren danke ich Joshua Berlin und Cristopher Czaban für viele hilfreiche Gespräche und eine gute Einführung in die Thematik und den Umgang mit Großrechnern.

Zu guter Letzt möchte ich noch Anja Höfling, Lars Fröhlich Wagenbach und meinen Eltern für den mentalen Rückhalt und das teilweise Korrekturlesen danken, genauso wie meinen Kommilitonen und Freunden Annabelle Uenver-Thiele, Constantin Butzke und Philipp Wolf für die kontinuierliche Unterstüzung während meines gesamten bisherigen Studiums.